

An efficient pressure-based methodology for low Mach flow simulations

Pascal Bruel

Centre National de la Recherche Scientifique (CNRS)

(pascal.bruel@univ-pau.fr)

(Univ Pau & Pays Adour/ E2S UPPA, Laboratoire de Mathématiques et de leurs Applications de Pau – Fédération IPRA, UMR5142 64000, Pau, France and Cagire team, Inria Bordeaux Sud-Ouest, France)

Congreso Argentino de Ingeniería Aeronáutica 2018

Córdoba - Argentina

November 2018



Where is Pau ????

France (European Union)

Population: 65 821 000 (2014)

Surface: 632 834 km²



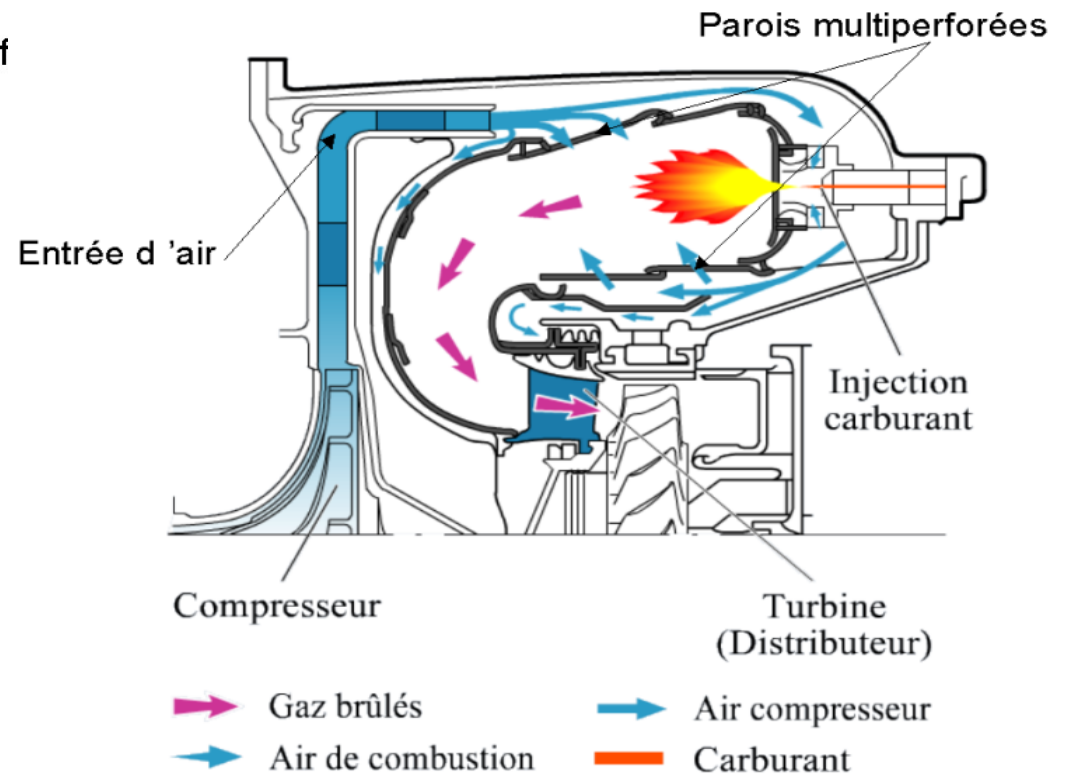
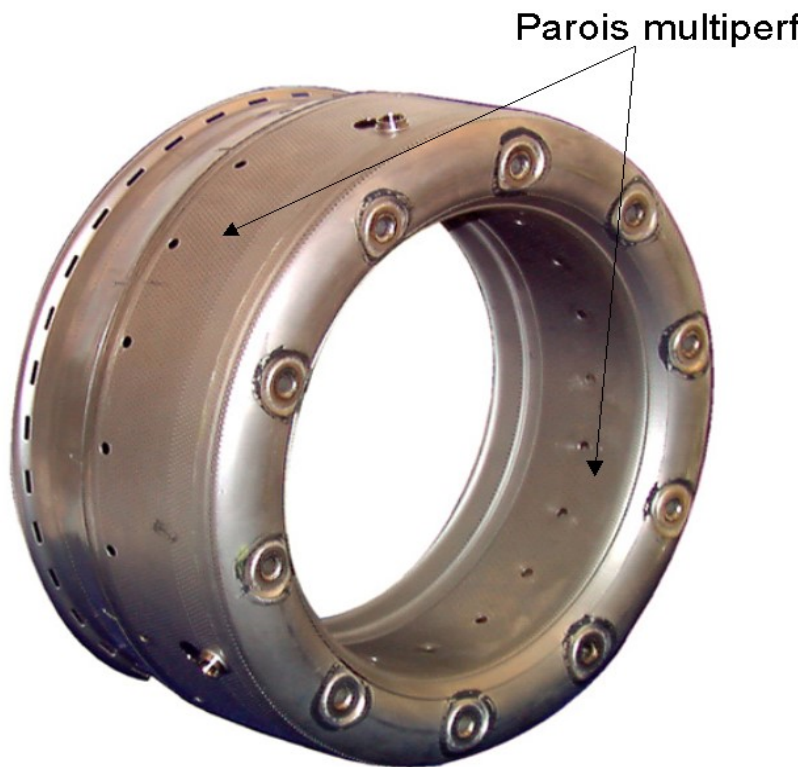
Pau University (~ 10000 students)

Presentation Layout

1. Introduction: examples of a low Mach flow configuration of interest.
2. Low Mach flows: a better insight about the major players with the asymptotic expansion of the governing equations.
3. A proposition of an efficient pressure-based method for low order co-located FV method.
4. Conclusion.

Example of a low Mach flow configuration:
from an aeronautical combustor to a baseline lab configuration

Example of a low Mach flow configuration



Aeronautical combustion chamber

Example of a low Mach flow configuration

→ Acoustic sources

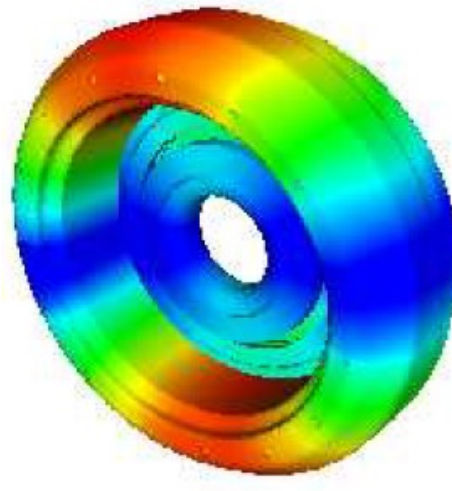
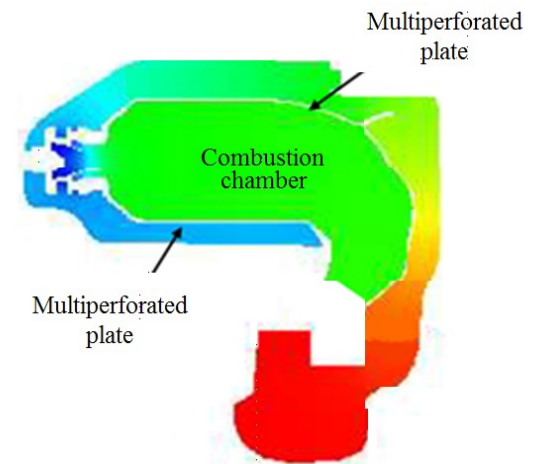
- Combustion noise (up to 80dB)
- Thermoacoustic instabilities (up to 140dB)
- Mechanical vibrations
- ...

→ Acoustic modes:

- Longitudinal
- Radial
- Azimuthal

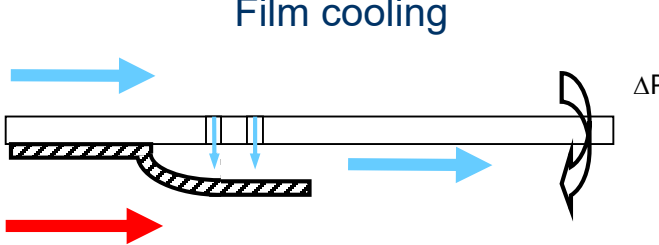
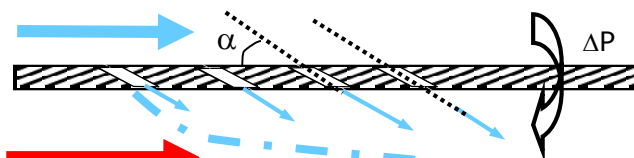
→ Wave types:

- Steady (all modes)
- Propagating (azimuthal modes essentially)



Example of a low Mach flow configuration

► Different wall cooling approaches

<p>Film cooling</p> 	<ul style="list-style-type: none">😊 Easy to manufacture😢 Short protection length
<p>Double wall</p> 	<ul style="list-style-type: none">😊 No local perturbation of the flow😢 Modest cooling efficiency
<p>Multiperforations</p> 	<ul style="list-style-type: none">😊 High cooling efficiency over the perforated plate😢 Important flow rate (~30% of total air supplied to the chamber)

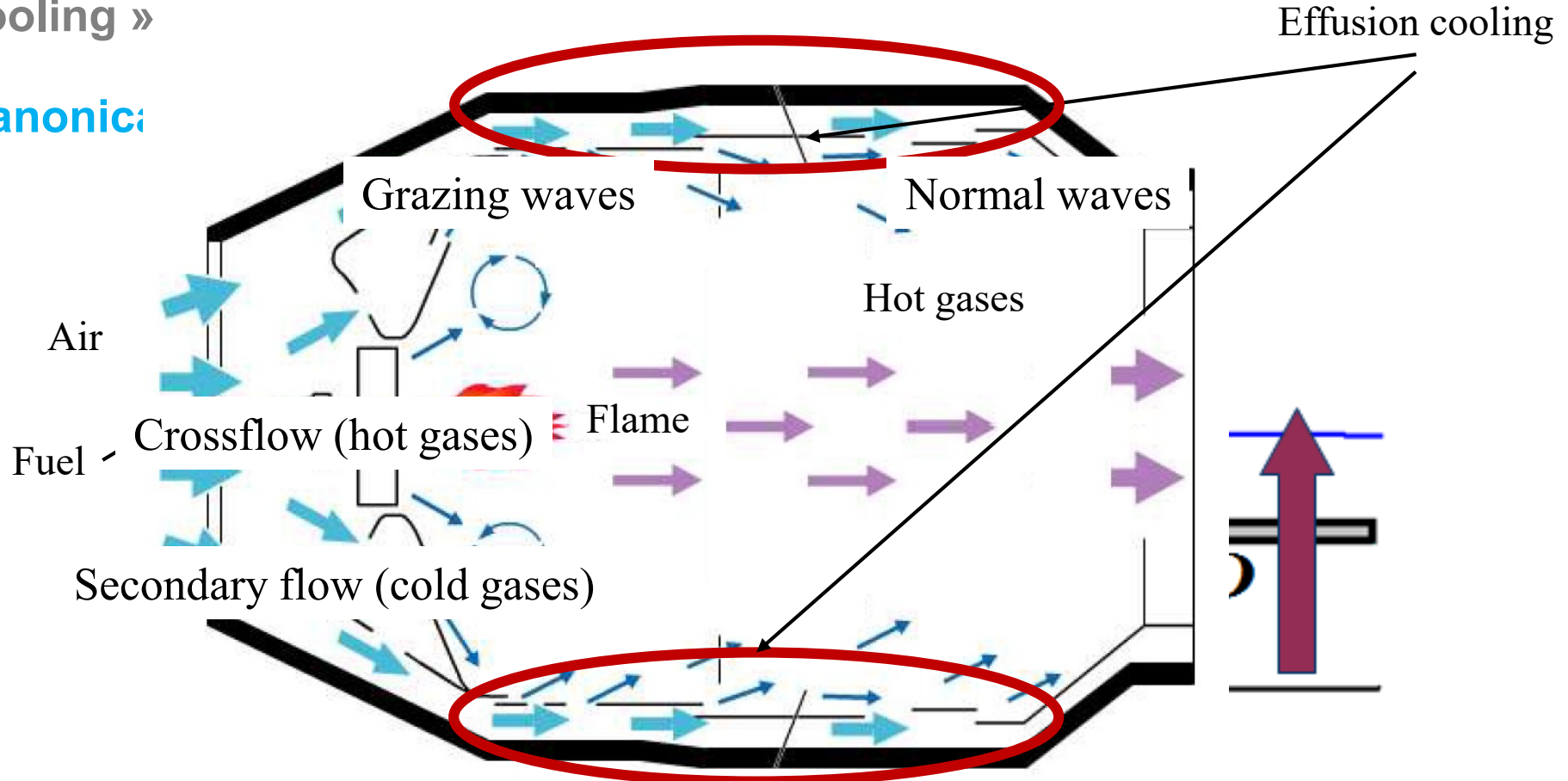
→ Hot gases ($\approx 2200\text{K}$) → Cooling air ($\approx 600\text{K}$)

←

Example of a low Mach flow configuration

→ Combustion chamber cooling through multiperforated surfaces « effusion cooling »

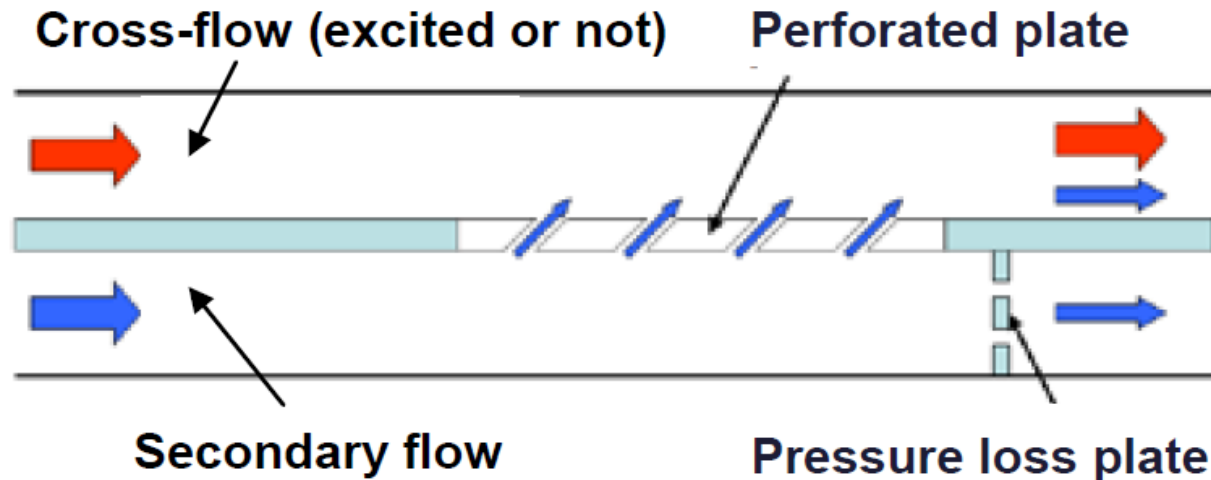
→ Canonical



Example of a low Mach flow configuration

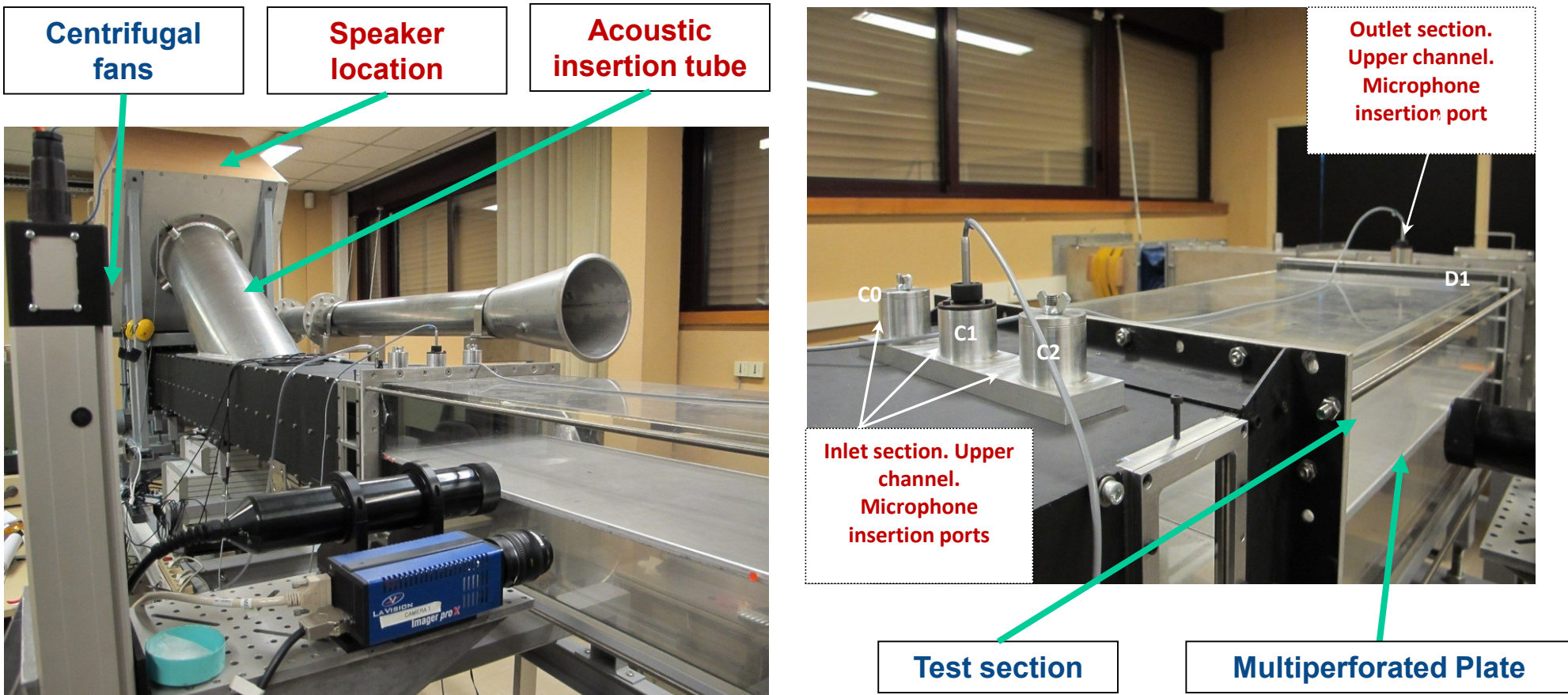
From a real combustor to a baseline lab configuration: the test bench MAVERIC

(A Multi-purpose rig for Accurate Validation by Experiments of Research on Innovative Cooling)



- " Two parallel turbulent channel flows
- " Multiperforated Plate → porosity 13,9%
- " Pressure Loss Plate → maximum porosity 25%

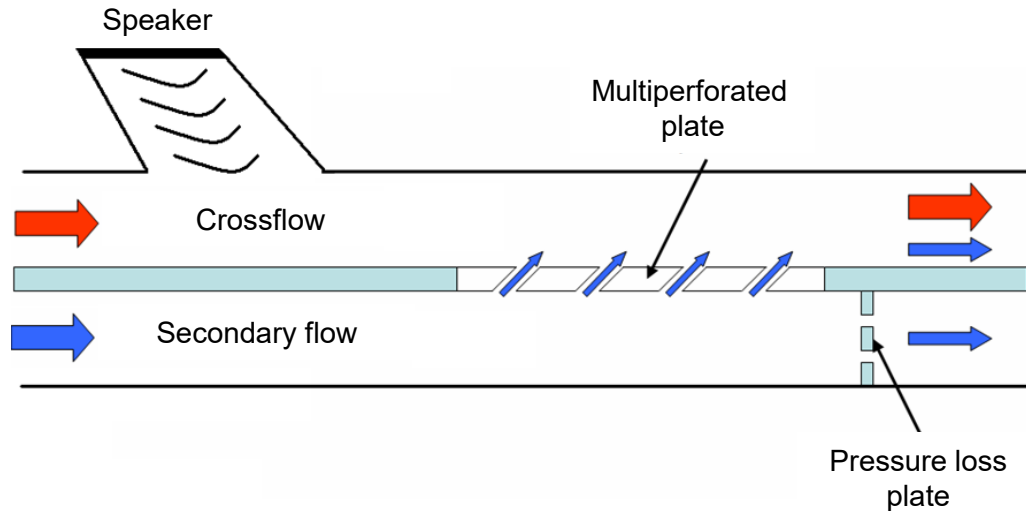
Example of a low Mach flow configuration



- " Pressure drop between lower and upper channel [10 – 140] Pa
- " Main stream Reynolds number [2000 – 35000] - Jet Reynolds number [1200 – 9000]
- " Typical Mach number values 10^{-3} – 10^{-2}

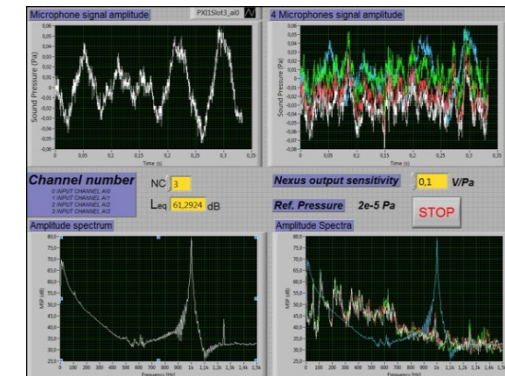
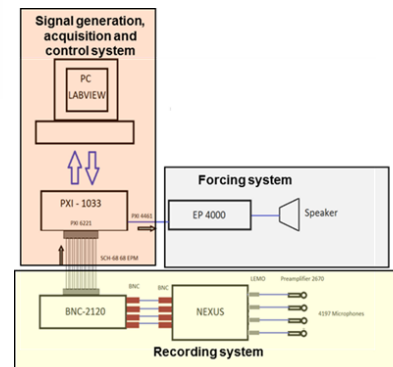
Example of a low Mach flow configuration

" With an acoustic excitation of the crossflow



Analysis of test bench acoustic response

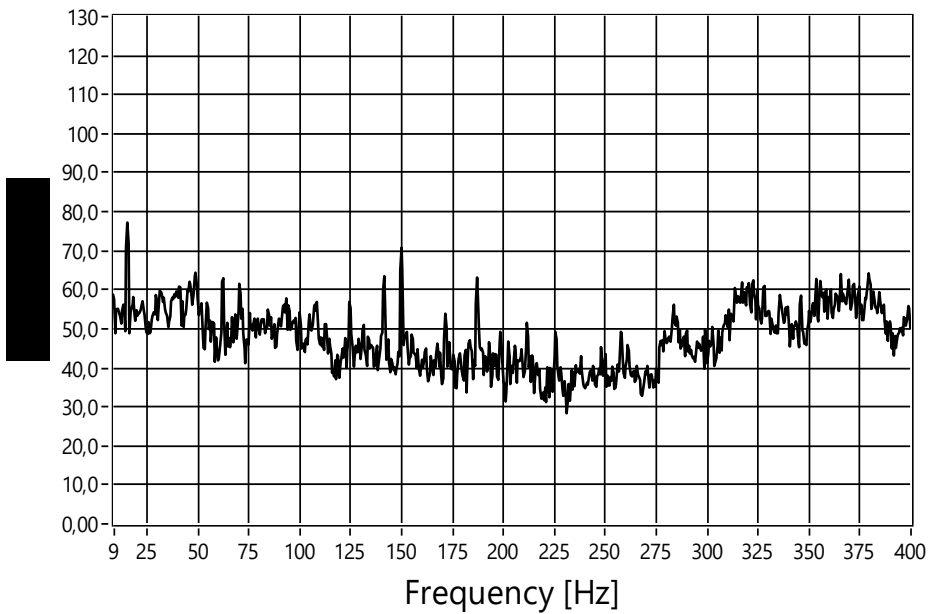
→ Development of data acquisition system and forcing system (LABVIEW)



- Setting-up of automatic displacement system for optic measurement tools.
- Laser Doppler Velocimetry (LDV) & Phase-Locked Particle image Velocimetry (PIV) measurements

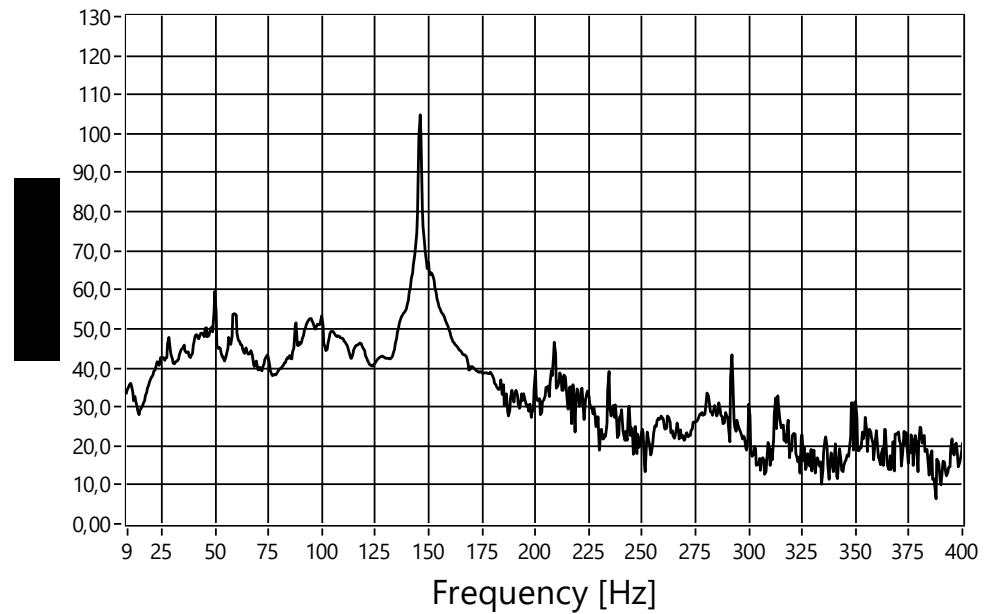
Example of a low Mach flow configuration

DP' Amplitude spectrum



No forcing

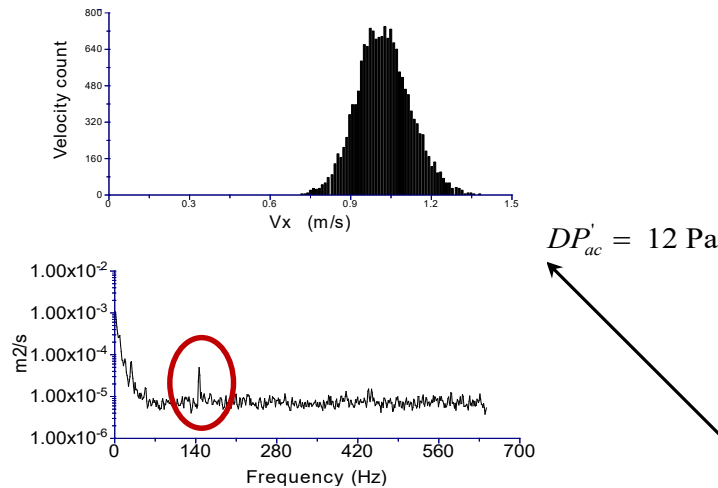
DP' Amplitude spectrum



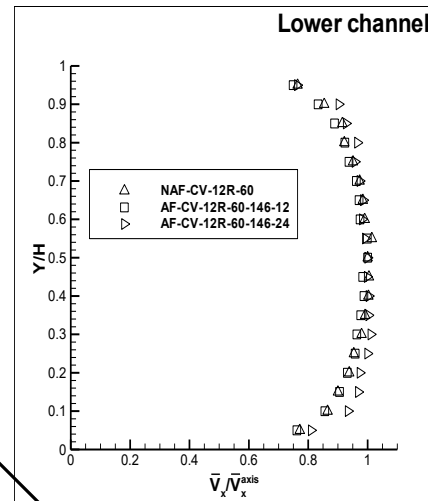
Forcing @146 Hz

SPECTRA OF THE UPSTREAM PARIETAL PRESSURE DIFFERENCE

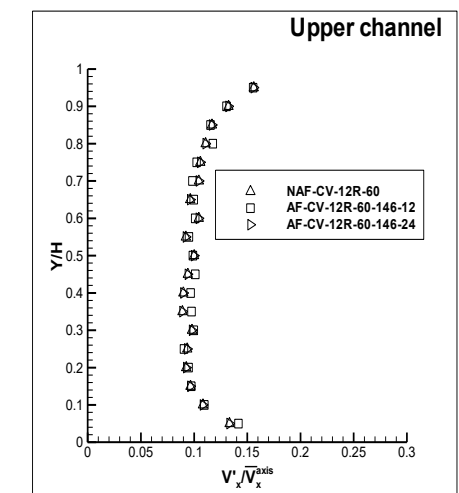
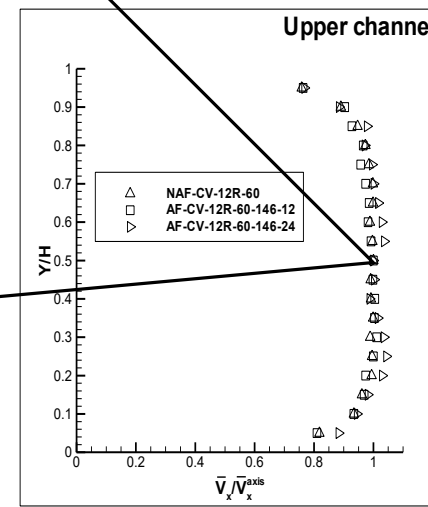
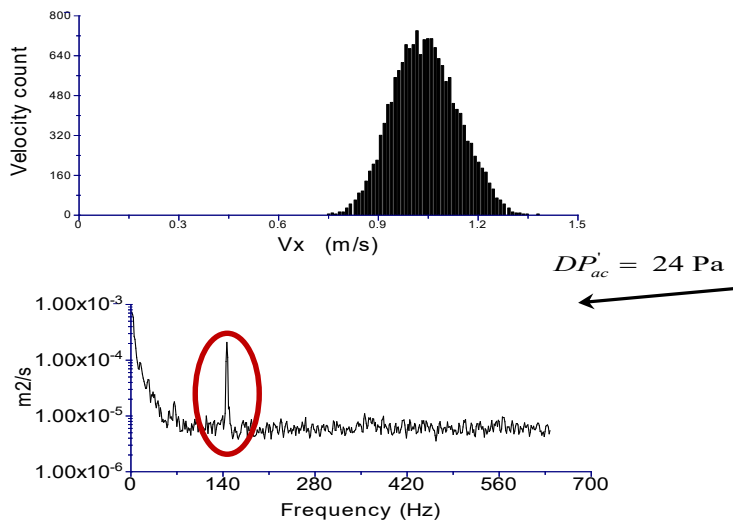
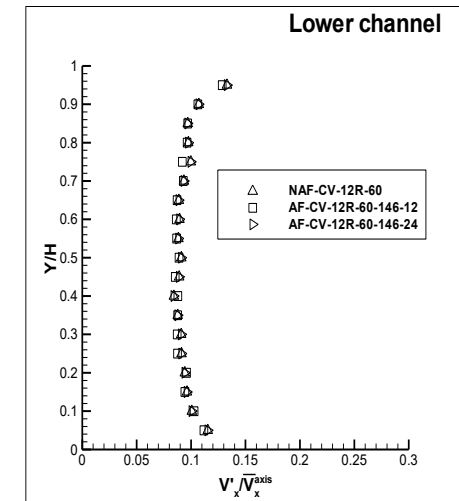
Example of a low Mach flow configuration



Streamwise velocity component spectra (right) and the related histograms (left) in the inlet upper channel



$@ X_1^* = -22.1 \text{ and } Y^* = 0.5$



Example of a low Mach flow configuration

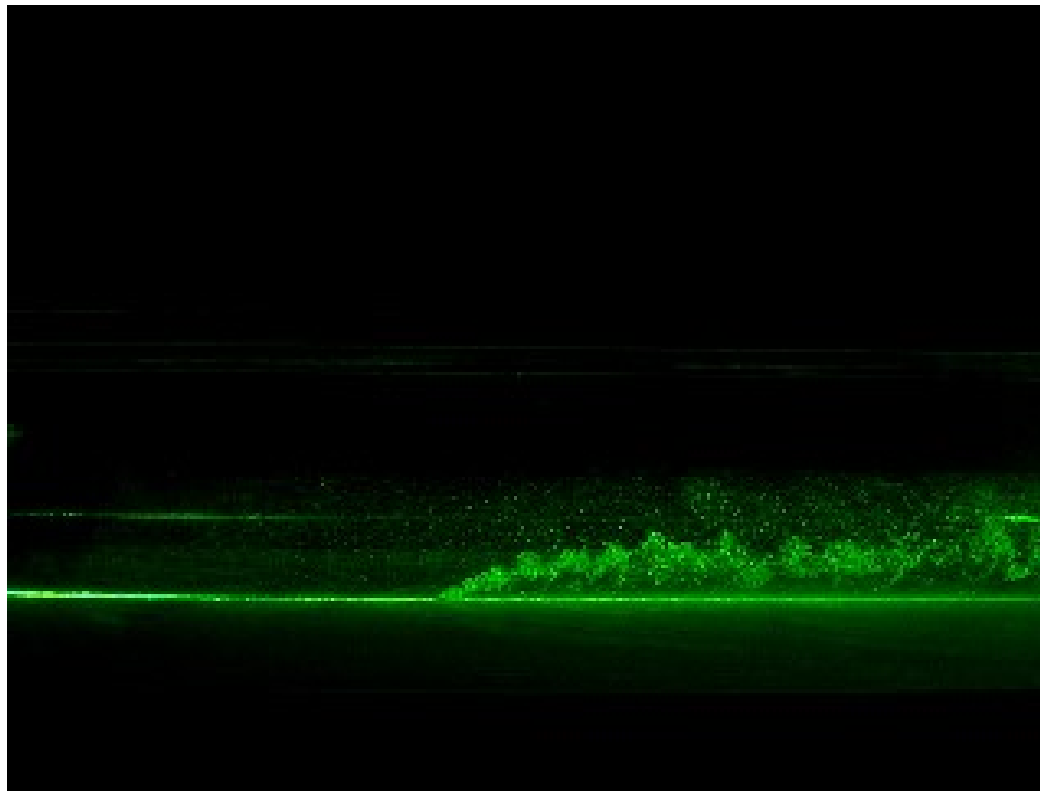
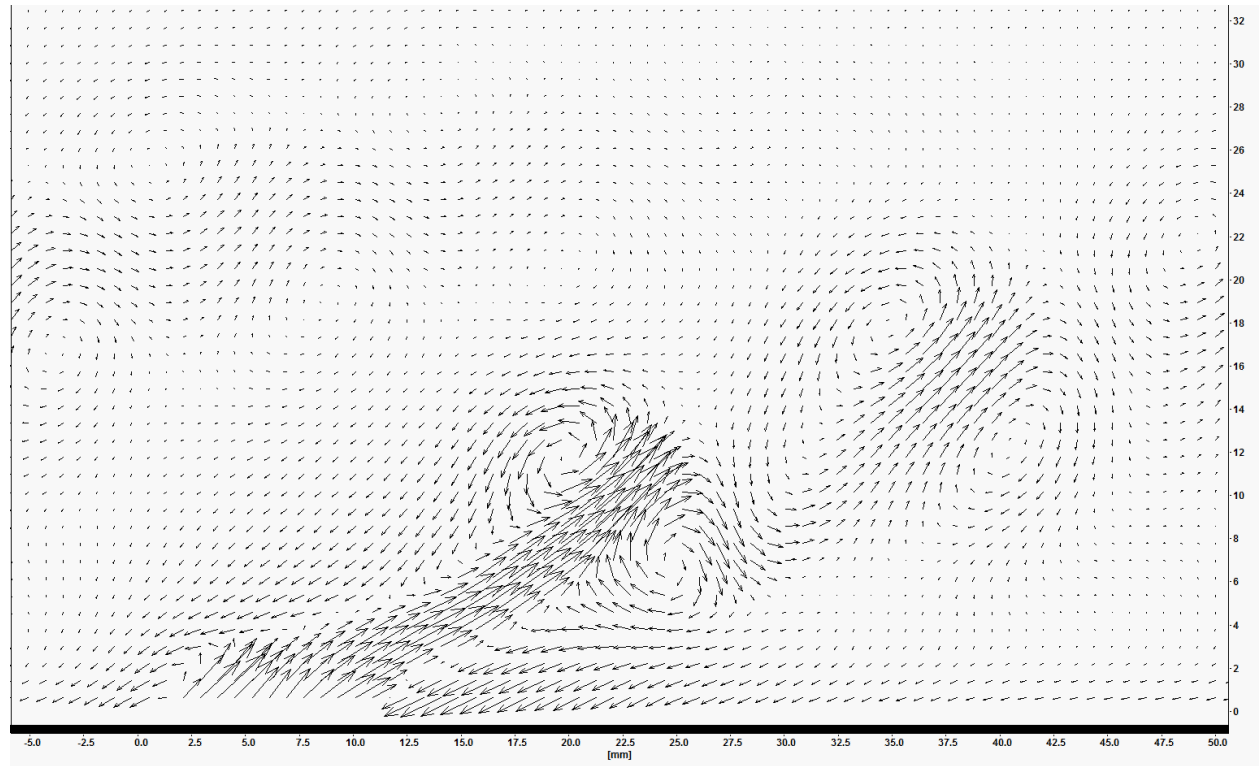


Illustration of the interaction between acoustics and hydrodynamics: visualization of a single jet in an excited crossflow @146 Hz

Example of a low Mach flow configuration

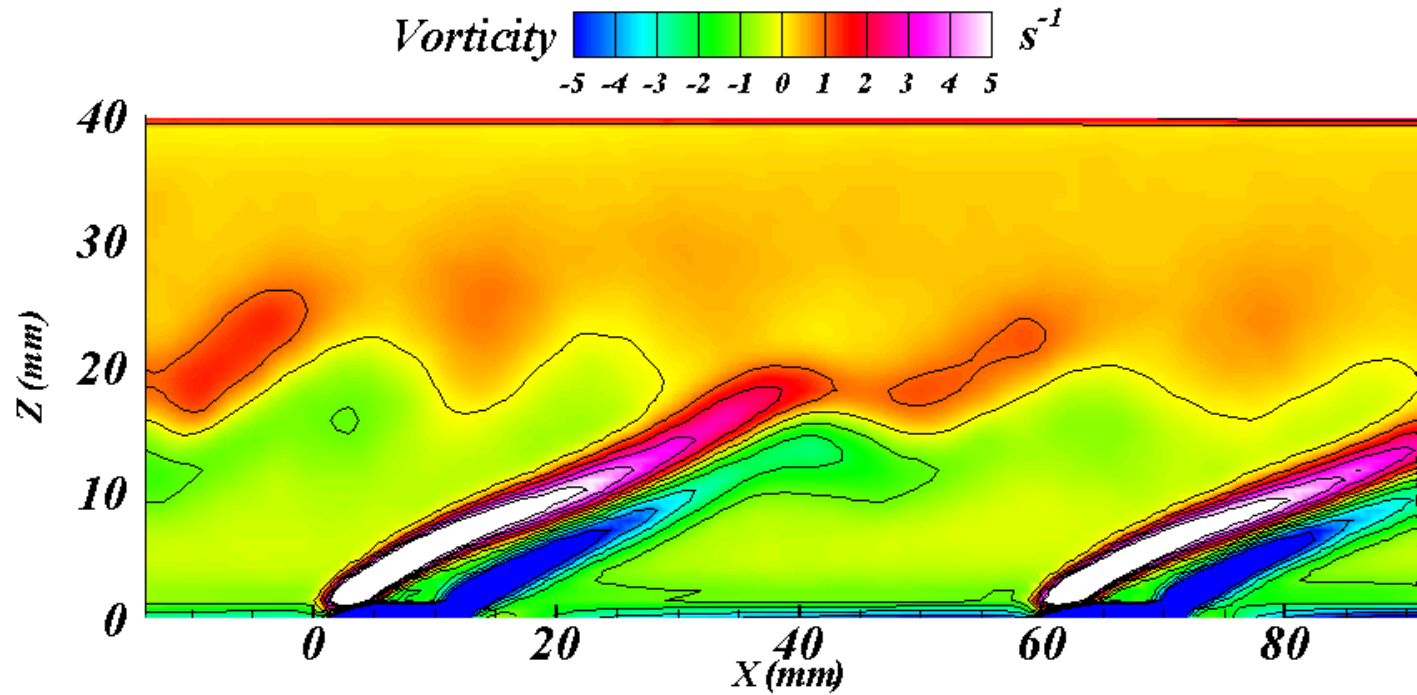
Examples of extraction of the jets' coherent motion: 2-component velocity



MAVERIC database - AF-CV-12R-60-146-24 , central jet of row 5: phase average time variation of velocity incorporating four phase locked averages (0° , 90° , 180° and 270° , (PIV, statistics over 600 images per phase angle).

Example of a low Mach flow configuration

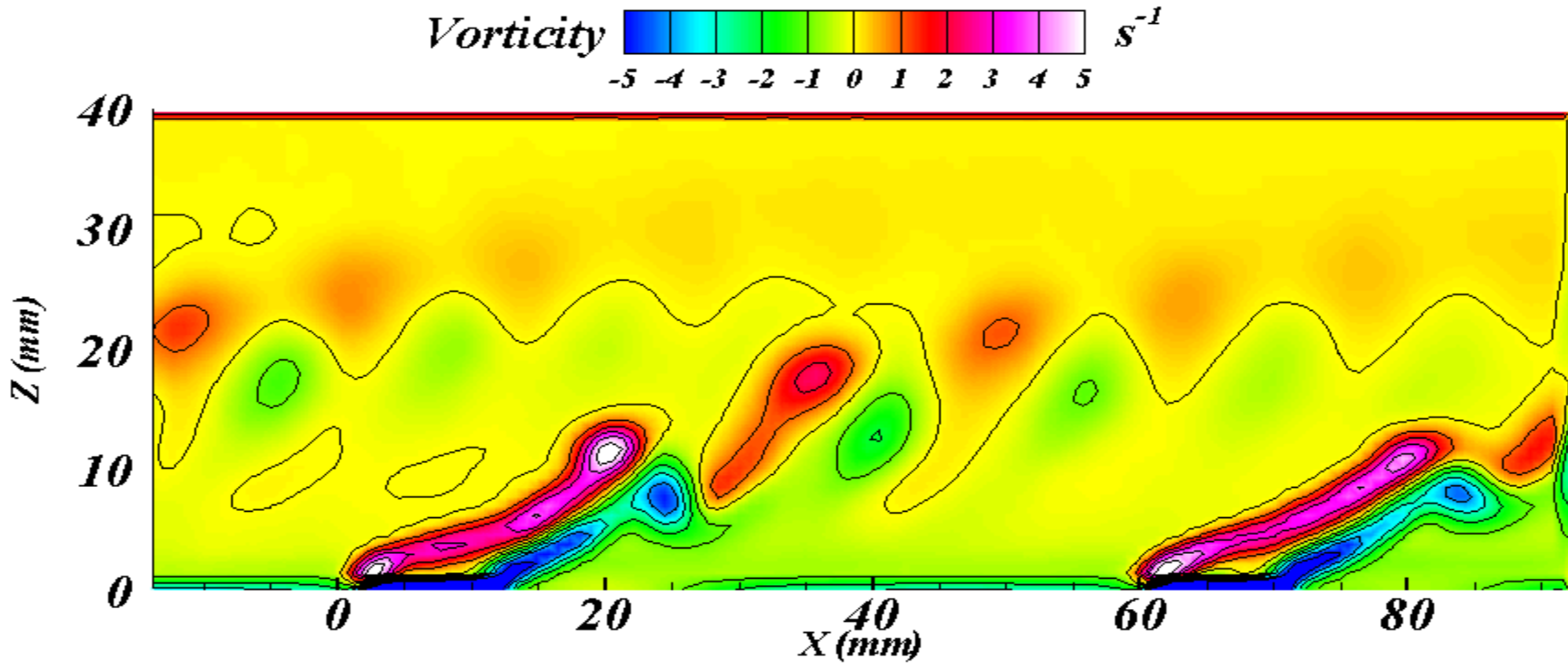
Examples of extraction of the jets' coherent motion: normal vorticity component



MAVERIC database - AF-CV-12R-60-146-24 , central jet of rows 3 and 5:
phase average time variation of vorticity incorporating four phase locked
averages (0° , 90° , 180° and 270° , (statistics over 600 images per phase
angle).

Example of a low Mach flow configuration

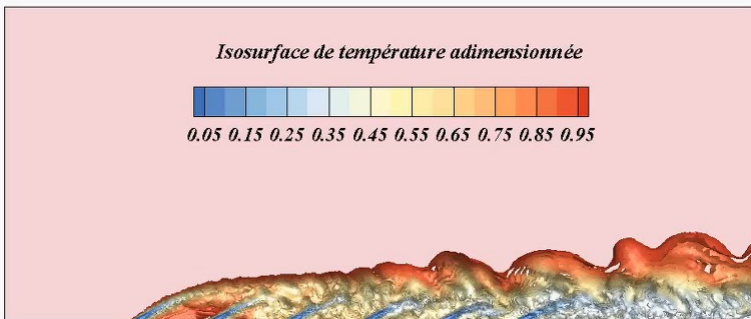
If the relative intensity of the forcing is increased by reducing the mean pressure drop from 60 Pa to 15 Pa



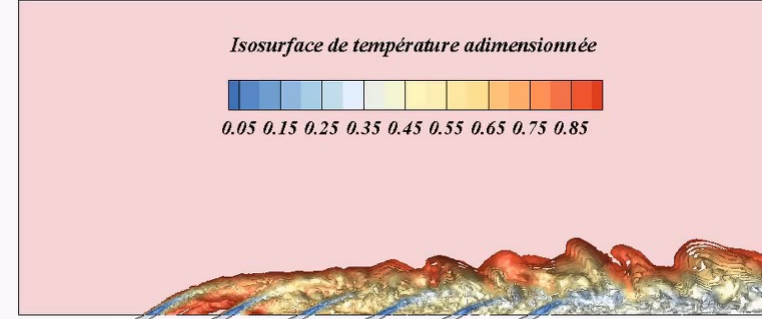
MAVERIC database - AF-CV-12R-15-146-24 , central jet of rows 3 and 5:
examples of extraction of the jet coherent motion: phase average time variation
incorporating four phase locked averages (0° , 90° , 180° and 270° , (statistics
over 600 images per phase angle).

LES computations with the explicit density based solver AVBP (Cerfacs & IFPEN): cumbersome and request large computing ressources

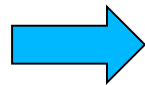
No crossflow excitation



With crossflow excitation



PhD thesis of Florenciano
(2013, Pau University)



Motivation for developing a low
Mach pressure-based approach

Low Mach flows: a better insight about the major players with an asymptotic expansion of the governing equations

Compressible Euler equations for a polytropic ideal gas: dimensionless form (Müller, VKI lectures, 1999):

$$\frac{t_{conv}}{t_{ref}} \frac{\partial \rho^*}{\partial t^*} + \nabla^* \cdot (\rho^* \mathbf{u}^*) = 0$$

$$\frac{t_{conv}}{t_{ref}} \frac{\partial \rho^* \mathbf{u}^*}{\partial t^*} + \nabla^* \cdot (\rho^* \mathbf{u}^* \otimes \mathbf{u}^*) = -\frac{1}{\hat{M}^2} \nabla^* p^*$$

$$\frac{t_{conv}}{t_{ref}} \frac{\partial \rho^* E^*}{\partial t^*} + \nabla^* \cdot (\rho^* \mathbf{u}^* H^*) = 0$$

with :

$$\rho^* = \rho / \rho_{ref}; p^* = p / p_{ref}; \mathbf{u}^* = \mathbf{u} / u_{ref}; \nabla^* = L_{ref} \nabla$$

$$t^* = t / t_{ref}; t_{conv} = L_{ref} / u_{ref}; E^* = E / (p_{ref} / \rho_{ref}); e^* = e / (p_{ref} / \rho_{ref}); H^* = H / (p_{ref} / \rho_{ref})$$

$$E^* = e^* + \frac{1}{2} \hat{M}^2 \|\mathbf{u}^*\|^2; H^* = E^* + \frac{p^*}{\rho^*}; p^* = \rho^* T^*; T^* = (\gamma - 1) e^*$$

$$\hat{M} = \sqrt{\gamma} \frac{u_{ref}}{\sqrt{\gamma p_{ref} / \rho_{ref}}} = \sqrt{\gamma} M_{ref}$$

Remark: u_{ref} is the reference convective velocity

$c_{ref} = \sqrt{\gamma p_{ref} / \rho_{ref}}$ is the reference speed of sound

One-scale expansion

The reference Mach number is chosen as the small parameter

From now on, we shall drop the superscript * for denoting the dimensionless variables and it is assumed that the low Mach number asymptotic analysis can be considered as a regular perturbation.

So each independent variables is expanded in terms of a series $\delta^{(i)}(\hat{M})$ where \hat{M} is the small parameter, for instance:

$$p(x, t; \hat{M}) = \delta^{(0)}(\hat{M}) p^{(0)}(x, t) + \delta^{(1)}(\hat{M}) p^{(1)}(x, t) + \delta^{(2)}(\hat{M}) p^{(2)}(x, t) + \dots$$

$$u(x, t; \hat{M}) = \delta^{(0)}(\hat{M}) u^{(0)}(x, t) + \delta^{(1)}(\hat{M}) u^{(1)}(x, t) + \delta^{(2)}(\hat{M}) u^{(2)}(x, t) + \dots$$

$$\rho(x, t; \hat{M}) = \delta^{(0)}(\hat{M}) \rho^{(0)}(x, t) + \delta^{(1)}(\hat{M}) \rho^{(1)}(x, t) + \delta^{(2)}(\hat{M}) \rho^{(2)}(x, t) + \dots$$

the scaling functions are chosen such that:

$$\delta^{(i)}(\hat{M}) = \hat{M}^i$$

Methodology : inject these expansions into the governing equations and order the power of \hat{M} .

One-scale asymptotics of the Euler equations: the hydrodynamic limit

Choose $t_{ref} = (L_{ref} / u_{ref})$

So $t_{ref} = t_{conv}$ is the **convective** time scale, the dimensionless system reads now as:

$$\frac{\partial \rho}{\partial t} + \nabla \cdot (\rho \mathbf{u}) = 0$$

$$\frac{\partial \rho \mathbf{u}}{\partial t} + \nabla \cdot (\rho \mathbf{u} \otimes \mathbf{u}) = -\frac{1}{\hat{M}^2} \nabla p$$

$$\frac{\partial \rho E}{\partial t} + \nabla \cdot (\rho \mathbf{u} H) = 0$$

One-scale asymptotics of the Euler equations: the hydrodynamic limit

By injecting the AD of each variable into the momentum equation →

$$\begin{aligned} \frac{\partial}{\partial t} & \left[(\rho^{(0)} + \rho^{(1)} \hat{\mathbf{M}} + \rho^{(2)} \hat{\mathbf{M}}^2) (\mathbf{u}^{(0)} + \mathbf{u}^{(1)} \hat{\mathbf{M}} + \mathbf{u}^{(2)} \hat{\mathbf{M}}^2) \right] + \\ & \nabla \cdot \left[(\rho^{(0)} + \rho^{(1)} \hat{\mathbf{M}} + \rho^{(2)} \hat{\mathbf{M}}^2) (\mathbf{u}^{(0)} + \mathbf{u}^{(1)} \hat{\mathbf{M}} + \mathbf{u}^{(2)} \hat{\mathbf{M}}^2) \otimes (\mathbf{u}^{(0)} + \mathbf{u}^{(1)} \hat{\mathbf{M}} + \mathbf{u}^{(2)} \hat{\mathbf{M}}^2) \right] = \\ & - \frac{1}{\hat{\mathbf{M}}^2} \nabla (p^{(0)} + p^{(1)} \hat{\mathbf{M}} + p^{(2)} \hat{\mathbf{M}}^2) \end{aligned}$$

One-scale asymptotics of the Euler equations: the hydrodynamic limit

Then, the momentum equation reads as (keeping only the leading terms):

$$\frac{\partial}{\partial t} \left[\rho^{(0)} \mathbf{u}^{(0)} \right] + \nabla \cdot (\rho^{(0)} \mathbf{u}^{(0)} \otimes \mathbf{u}^{(0)}) = -\nabla p^{(2)} - \hat{M}^{-1} \nabla p^{(1)} - \hat{M}^{-2} \nabla p^{(0)}$$

to be satisfied for all \hat{M} when $\hat{M} \rightarrow 0$

so:

$$\text{Term } \hat{M}^{-2} \rightarrow \nabla p^{(0)} = 0 \Leftrightarrow p^{(0)}(\mathbf{x}, t) = p^{(0)}(t)$$

$$\text{Term } \hat{M}^{-1} \rightarrow \nabla p^{(1)} = 0 \Leftrightarrow p^{(1)}(\mathbf{x}, t) = p^{(1)}(t)$$

$$\text{Term } \hat{M}^0 \rightarrow \frac{\partial}{\partial t} \left[\rho^{(0)} \mathbf{u}^{(0)} \right] + \nabla \cdot (\rho^{(0)} \mathbf{u}^{(0)} \otimes \mathbf{u}^{(0)}) = -\nabla p^{(2)}$$

One-scale asymptotics of the Euler equations: the hydrodynamic limit

Doing the same for the continuity and the energy equation leads to the final system for $O(1)$ variables which reads as:

$$\frac{\partial \rho^{(0)}}{\partial t} + \nabla \cdot (\rho^{(0)} \mathbf{u}^{(0)}) = 0$$

$$\frac{\partial \rho^{(0)} \mathbf{u}^{(0)}}{\partial t} + \nabla \cdot (\rho^{(0)} \mathbf{u}^{(0)} \otimes \mathbf{u}^{(0)}) = -\nabla p^{(2)}$$

$$\frac{\gamma}{\gamma-1} \rho^{(0)} \left[\frac{\partial T^{(0)}}{\partial t} + \mathbf{u}^{(0)} \cdot \nabla \cdot T^{(0)} \right] = \frac{dp^{(0)}}{dt}$$

$$\rho^{(0)}(x, t) T^{(0)}(x, t) = p^{(0)}(t)$$

One-scale asymptotics of the Euler equations: the hydrodynamic limit

With periodic boundary conditions, the kinetic energy defined
by:

$$E_{\text{kin}} = \int_{\mathbb{T}_{\text{advect}}} \frac{1}{2} \varrho^{(0)} \|\boldsymbol{v}^{(0)}\|^2.$$

remains constant in time

One-scale asymptotics of the Euler equations: the acoustic limit

Choose now $t_{ref} = (L_{ref} / (c_{ref} / \sqrt{\gamma}))$

So $t_{ref} = t_{ac}$ is now an **acoustic** time scale, the dimensionless system reads now as:

$$\frac{1}{\hat{M}} \frac{\partial \rho}{\partial t} + \nabla \cdot (\rho \mathbf{u}) = 0$$

$$\frac{1}{\hat{M}} \frac{\partial \rho \mathbf{u}}{\partial t} + \nabla \cdot (\rho \mathbf{u} \otimes \mathbf{u}) = -\frac{1}{\hat{M}^2} \nabla p$$

$$\frac{1}{\hat{M}} \frac{\partial \rho E}{\partial t} + \nabla \cdot (\rho \mathbf{u} H) = 0$$

One-scale asymptotics of the Euler equations: the acoustic limit

By injecting the AD of each variable into the momentum equation \rightarrow

$$\begin{aligned} \frac{1}{\hat{M}} \frac{\partial}{\partial t} & \left[(\rho^{(0)} + \rho^{(1)} \hat{M} + \rho^{(2)} \hat{M}^2) (\mathbf{u}^{(0)} + \mathbf{u}^{(1)} \hat{M} + \mathbf{u}^{(2)} \hat{M}^2) \right] + \\ \nabla \cdot & \left[(\rho^{(0)} + \rho^{(1)} \hat{M} + \rho^{(2)} \hat{M}^2) (\mathbf{u}^{(0)} + \mathbf{u}^{(1)} \hat{M} + \mathbf{u}^{(2)} \hat{M}^2) \otimes (\mathbf{u}^{(0)} + \mathbf{u}^{(1)} \hat{M} + \mathbf{u}^{(2)} \hat{M}^2) \right] = \\ -\frac{1}{\hat{M}^2} \nabla & (p^{(0)} + p^{(1)} \hat{M} + p^{(2)} \hat{M}^2) \end{aligned}$$

One-scale asymptotics of the Euler equations: the acoustic limit

Then, the momentum equation reads as (keeping only the three leading terms):

$$\begin{aligned} \frac{\partial}{\partial t} \left[\rho^{(1)} \mathbf{u}^{(0)} \right] + \frac{\partial}{\partial t} \left[\rho^{(0)} \mathbf{u}^{(1)} \right] + \nabla \cdot (\rho^{(0)} \mathbf{u}^{(0)} \otimes \mathbf{u}^{(0)}) = \\ -\nabla p^{(2)} - \hat{M}^{-1} \left(\nabla p^{(1)} + \frac{\partial}{\partial t} \rho^{(0)} \mathbf{u}^{(0)} \right) - \hat{M}^{-2} \nabla p^{(0)} \end{aligned}$$

to be satisfied for all \hat{M} when $\hat{M} \rightarrow 0$

so:

$$\text{Term } \hat{M}^{-2} \rightarrow \nabla p^{(0)} = 0 \Leftrightarrow p^{(0)}(\mathbf{x}, t) = p^{(0)}(t)$$

$$\text{Term } \hat{M}^{-1} \rightarrow \nabla p^{(1)} + \frac{\partial}{\partial t} \rho^{(0)} \mathbf{u}^{(0)} = 0$$

$$\text{Term } \hat{M}^0 \rightarrow \frac{\partial}{\partial t} (\rho \mathbf{u})^{(1)} + \nabla \cdot (\rho^{(0)} \mathbf{u}^{(0)} \otimes \mathbf{u}^{(0)}) = -\nabla p^{(2)}$$

One-scale asymptotics of the Euler equations: the acoustic limit

Then, the continuity equation reads as (keeping only the leading terms):

$$\frac{\partial}{\partial t} \rho^{(1)} + \nabla \cdot (\rho^{(0)} \mathbf{u}^{(0)}) + \hat{M}^{-1} \frac{\partial}{\partial t} \rho^{(0)} = 0$$

to be satisfied for all \hat{M} when $\hat{M} \rightarrow 0$

so:

$$\text{Term } \hat{M}^{-1} \rightarrow \frac{\partial}{\partial t} \rho^{(0)} = 0$$

$$\text{Term } \hat{M}^0 \rightarrow \frac{\partial}{\partial t} \rho^{(1)} + \nabla \cdot (\rho^{(0)} \mathbf{u}^{(0)}) = 0$$

combined with the energy equation it yields after some algebra the **linear acoustic equations**:

$$\left\{ \begin{array}{l} \rho^{(0)} \frac{\partial}{\partial t} \mathbf{u}^{(0)} + \nabla p^{(1)} = 0 \\ \frac{\partial}{\partial t} p^{(1)} + \rho^{(0)} c_0^2 \nabla \cdot \mathbf{u}^{(0)} = 0 \text{ with } c_0^2 = \gamma p^{(0)} / \rho^{(0)} \end{array} \right.$$

One-scale asymptotics of the Euler equations: the acoustic limit

With periodic boundary conditions, the acoustic energy defined by:

$$E_{\text{acoust}} = \int_{\mathbb{T}_{\text{acoust}}} \left[\frac{1}{2} \widetilde{\varrho^{(0)}} \|\widetilde{\mathbf{v}^{(0)}}\|^2 + \frac{1}{2} \frac{(p^{(1)})^2}{\widetilde{\varrho^{(0)}} (c^{(0)})^2} \right].$$

remains constant in time. Here, the tilde denotes an averaged value over a region of characteristic scale of $1/\hat{M}$

How to get a flavor of the interaction between acoustics and hydrodynamics ?  Two-scale expansion

Low Mach flows: asymptotic expansion of the governing equations

Using a single space scale and **two** time scales t / t_{conv} and t / t_{ac} , any field variable, for instance for the pressure, is expanded as:

$$p(x, t; \hat{M}) = p^{(0)}(x, t, \tau) + \hat{M} p^{(1)}(x, t, \tau) + \hat{M}^2 p^{(2)}(x, t, \tau) + O(\hat{M}^3)$$

with $t/t_{conv} \equiv t$ and $t / t_{ac} \equiv \tau$

The time derivative at constant x and \hat{M} yields (chain rule):

$$\frac{\partial}{\partial t} \Big|_{x, \hat{M}} = \frac{\partial}{\partial t} + \frac{1}{\hat{M}} \frac{\partial}{\partial \tau}$$

Low Mach flows: asymptotic expansion of the governing equations (Navier-Stokes)

After substitution, the zeroth, first and second order equations yield:

Continuity

$$\frac{\partial \rho^{(0)}}{\partial \tau} = 0 \Rightarrow \rho^{(0)} = \rho^{(0)}(\mathbf{x}, t)$$

$$\frac{\partial \rho^{(1)}}{\partial \tau} + \frac{\partial \rho^{(0)}}{\partial t} + \nabla \cdot (\rho \mathbf{u})^{(0)} = 0$$

$$\frac{\partial \rho^{(2)}}{\partial \tau} + \frac{\partial \rho^{(1)}}{\partial t} + \nabla \cdot (\rho \mathbf{u})^{(1)} = 0$$

Momentum

$$\nabla p^{(0)} = 0 \Rightarrow p^{(0)} = p^{(0)}(t)$$

$$\frac{\partial(\rho \mathbf{u})^{(0)}}{\partial \tau} = -\nabla p^{(1)} \Rightarrow \frac{\partial \mathbf{u}^{(0)}}{\partial \tau} = -\frac{1}{\rho^{(0)}} \nabla p^{(1)}$$

$$\frac{\partial(\rho \mathbf{u})^{(1)}}{\partial \tau} + \frac{\partial(\rho \mathbf{u})^{(0)}}{\partial t} + \nabla \cdot (\rho \mathbf{u} \otimes \mathbf{u})^{(0)} = -\nabla p^{(2)} + \frac{1}{\text{Re}} \nabla \cdot \boldsymbol{\tau}^{(0)}$$

Low Mach flows: asymptotic expansion of the governing equations (Here, the Navier-Stokes system with reaction)

Energy equation

$$\frac{\partial(\rho E)^{(0)}}{\partial \tau} = 0$$

$$\frac{\partial(\rho E)^{(1)}}{\partial \tau} + \frac{\partial(\rho E)^{(0)}}{\partial t} + \nabla \cdot (\rho \mathbf{u} H)^{(0)} = \frac{\gamma}{\gamma-1} \frac{1}{\text{Pr Re}} \nabla \cdot (\lambda \nabla T)^{(0)} + (\rho q)^{(0)}$$

$$\frac{\partial(\rho E)^{(2)}}{\partial \tau} + \frac{\partial(\rho E)^{(1)}}{\partial t} + \nabla \cdot (\rho \mathbf{u} H)^{(1)} = \frac{\gamma}{\gamma-1} \frac{1}{\text{Pr Re}} \nabla \cdot (\lambda \nabla T)^{(1)} + (\rho q)^{(1)}$$

State equations

$$\rho^{(0)}(t, x) T^{(0)}(t, x) = p^{(0)}(t)$$

$$p^{(0)}(t) = (\gamma - 1)(\rho E)^{(0)}(t)$$

Low Mach flows: a better insight about the major players with an asymptotic expansion of the governing equations (Navier-Stokes)

The first order energy equation can be also expressed as:

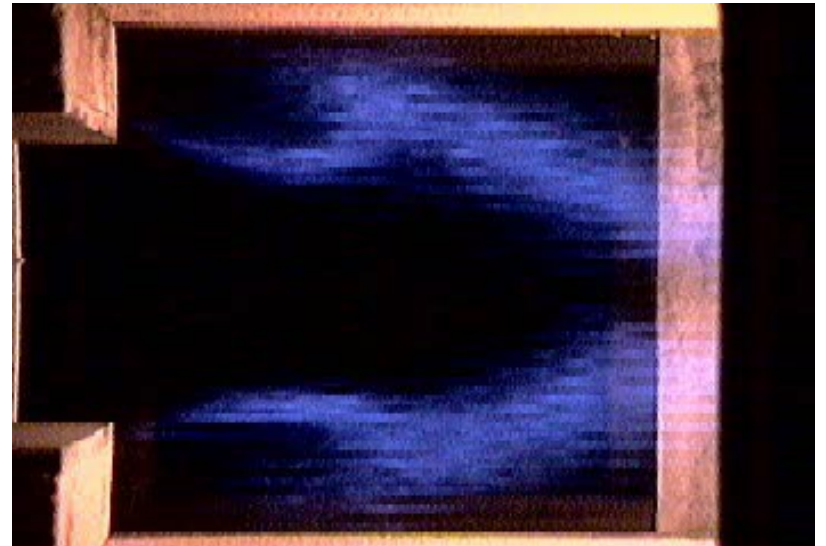
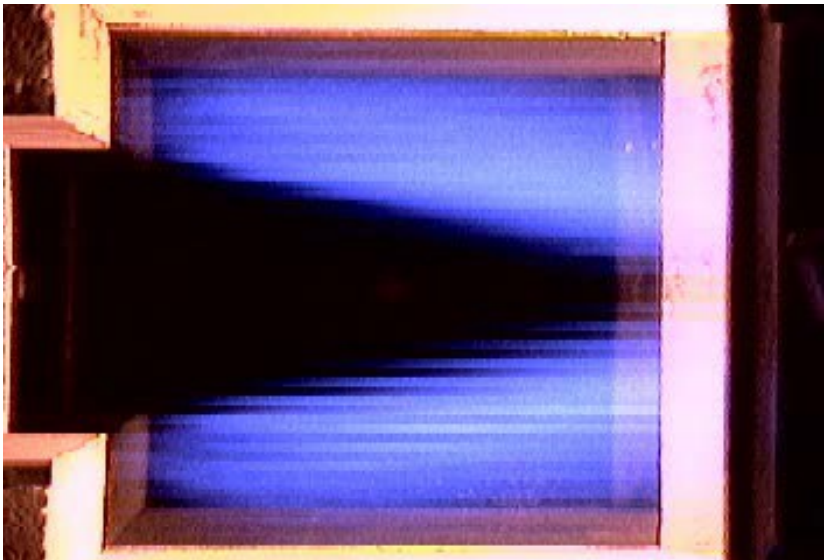
$$\frac{\partial p^{(1)}}{\partial \tau} + \gamma p^{(0)} \nabla \cdot (\mathbf{u})^{(0)} = \gamma \frac{1}{\text{Pr Re}} \nabla \cdot (\lambda \nabla T)^{(0)} + (\gamma - 1)(\rho q)^{(0)} - \frac{dp^{(0)}}{dt}$$

Differentiating the above equation with respect to τ and subtracting $\gamma p^{(0)}$ times the divergence of the first order momentum equation yields:

$$\frac{\partial^2 p^{(1)}}{\partial \tau^2} - \nabla \cdot (c^{(0)2} \nabla p^{(1)})^{(0)} = (\gamma - 1) \frac{\partial(\rho q)^{(0)}}{\partial \tau} \quad \text{with } c^{(0)2} = \gamma \frac{p^{(0)}(t)}{\rho^{(0)}(\mathbf{x}, t)}$$

This is a wave equation and its source is the change **over acoustic time** of the **leading order of the heat release rate**.

Low Mach flows: illustration of a reacting flows featuring turbulence and coherent motion related with thermoacoustic coupling



Turbulent premixed reaction zone stabilized
by a dump (from Nguyen et al., FTC 2003)

Important features of low Mach flows

A priori, the low Mach flow solution results from the superimposition/interaction of a slow component (with a quasi-like Mach zero behavior) **and** a fast component (acoustic waves).

The density may vary significantly in relation with the exact nature of the flow at hand (reacting flow).

Low Mach flows simulations: what are the choices ?

Density-based approach: preconditioning techniques, modification of the diffusion matrix of the flux scheme.

Pressure-based approach: this approach originally developed to cope with Mach zero flow must be adapted: the energy equation plays a key role (Klein, JCP 1995) and so will be used for establishing the pressure correction equation.

A pressure-based approach proposed for low Mach flow simulations

In close collaboration with Prof. E. Dick and Dr. Y. Moguen

Moguen, Y., Bruel, P., Dick, E. (2018) “*A parameter-free pressure-correction algorithm for simulation of convective and acoustic transport at all levels of Mach number*”. Journal of Computational Physics, submitted, under revision.

Moguen, Y., Bruel, P., Dick, E. (2015) ”*Solving low Mach number Riemann problems by a momentum interpolation method*”, Journal of Computational Physics, **298**:741-746.

Moguen, Y., Delmas, S., Perrier, V., Bruel, P., Dick, E. (2015) “*Godunov-type schemes with inertia terms for unsteady full Mach number range flow calculations*”, Journal of Computational Physics, **281**:556-590.

Moguen, Y., Bruel, P., Perrier, V., Dick, E. (2014) “*Non-reflective inlet conditions for the calculation of unsteady turbulent compressible flows at low Mach number*”, Mechanics and Industry, **15**(3):179-189.

Moguen, Y., Bruel, P., Dick, E., (2013) “*Semi-implicit characteristic-based boundary treatment for acoustics in low Mach number flows*”, Journal of Computational Physics, **255**:339-361.

Moguen, Y., Dick, E., Vierendeels, J., Bruel, P. (2013) “*Pressure-velocity coupling for unsteady low Mach number flow simulations: an improvement of the AUSM+-up scheme*”, Journal of Computational and Applied Mathematics, **246**:136-143.

Moguen, Y., Kousksou, T., Bruel, P., Vierendeels, J. and Dick, E. (2012) “*Pressure-velocity coupling allowing acoustic calculation in low Mach number flow*”, Journal of Computational Physics, **231**:5522-5541.

The continuous system of PDE's at hand: the Euler equations with a co-located formulation

$$\frac{\partial \rho}{\partial t} + \nabla \cdot (\rho \mathbf{u}) = 0$$

$$\frac{\partial \rho \mathbf{u}}{\partial t} + \nabla \cdot (\rho \mathbf{u} \otimes \mathbf{u}) = -\nabla p$$

$$\frac{\partial \rho E}{\partial t} + \nabla \cdot (\rho \mathbf{u} H) = 0$$

$$E = e + \frac{1}{2} \|\mathbf{u}\|^2 = c_v T + \frac{1}{2} \|\mathbf{u}\|^2; H = E + \frac{p}{\rho}$$

$$p = (\gamma - 1) \rho e$$

Together with proper initial and boundary conditions

Our proposition for the pressure-based algorithm: a predictor-corrector loop

Predictor step (pressure frozen): solving the continuity and the momentum equations.

Corrector step (density frozen): solving the energy equation to get the pressure correction with input from the momentum equation.

In both steps, the face values on the primal mesh are derived by the MIAU flux scheme

Main ingredients of a pressure-based algorithm within a co-located finite volume framework

1. Expressions of the face velocity and the face pressure.
2. Equation(s) at the source of the derivation of the pressure correction.

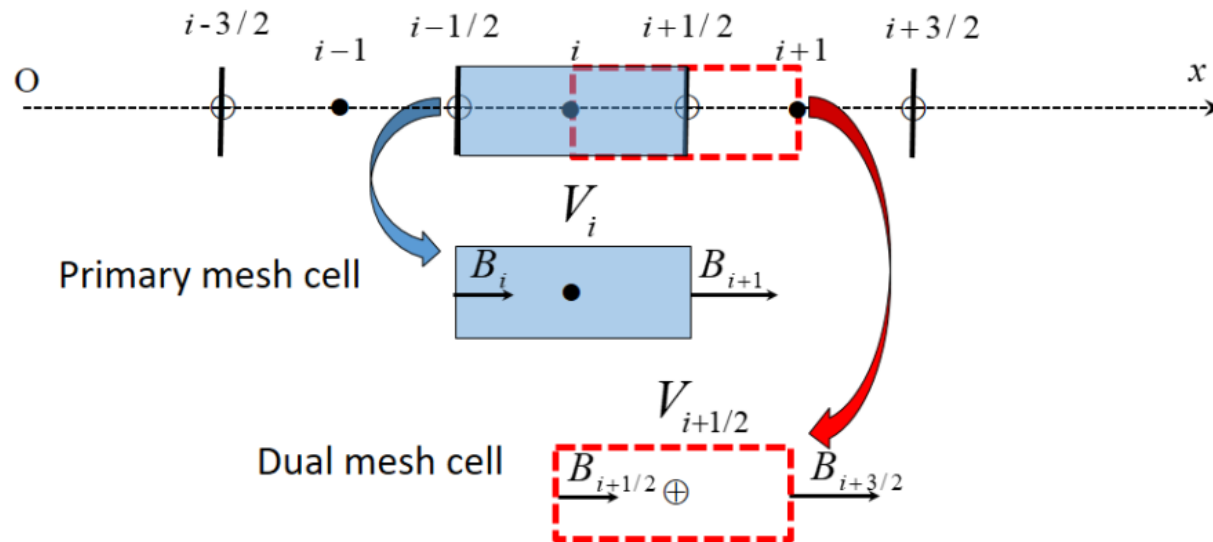
Expression of the face velocity

The transporting velocity is given a **dynamical meaning** and so it is assumed that it satisfies an evolution equation obtained by discretizing the continuous momentum equation on the dual mesh → this is the starting point of the **momentum interpolation method**,

The momentum interpolation method in brief for the face velocity

Consider a first order Euler implicit time discretization of the momentum equation. Thus, the discrete equation at time $t_{n+1} = (n + 1)\Delta t$ reads as:

$$(\rho u)_i^{n+1} \approx \frac{\Delta t}{(x_{i+1/2} - x_{i-1/2})} \left[(\rho uu)_i^{n+1} - (\rho uu)_{i-1/2}^{n+1} + (p)_{i+1/2}^{n+1} - (p)_{i-1/2}^{n+1} \right]$$



The momentum interpolation method in brief for the face velocity

For the flux of momentum, let's re-write it formally as :

$$(\rho uu)_{i-1/2}^{n+1} = (\rho u)_{i-1/2}^{n+1} u_{i-1/2}^{n+1} \text{ and conversely } (\rho uu)_{i+1/2}^{n+1} = (\rho u)_{i+1/2}^{n+1} u_{i+1/2}^{n+1}$$

Then, consider that $(\rho u)_{i\pm 1/2}^{n+1}$ is the sought **transported** quantity and that $u_{i\pm 1/2}^{n+1}$ is the **transporting** velocity. On the ground of the sole discretization on the primal cell, $u_{i\pm 1/2}^{n+1}$ can be thought of as an interpolated quantity based on the cell based values .

The momentum interpolation method in brief for the face velocity

Then, the following choices are made:

- 1) The transporting velocity is treated explicitly in time (or in the predictor-corrector loop) so $u_{i\pm 1/2}^{n+1} \approx u_{i\pm 1/2}^n$
- 2) An upwind first order expression in space is retained for the transported quantity.

So one gets the following expressions (positive velocities):

$$(\rho uu)_{i-1/2}^{n+1} \approx (\rho u)_{i-1}^{n+1} u_{i-1/2}^n \stackrel{\text{notation}}{\equiv} B_i$$

$$(\rho uu)_{i+1/2}^{n+1} \approx (\rho u)_i^{n+1} u_{i+1/2}^n \stackrel{\text{notation}}{\equiv} (\rho u)_i^{n+1} A_i = B_{i+1}$$

The momentum interpolation method in brief for the face velocity

So, the B_i 's stand for the momentum flux at the interfaces of the primal mesh and the A_i 's stand for the transporting velocities therein, so with these notations, the discretized momentum equation on a primal mesh cell reads now as:

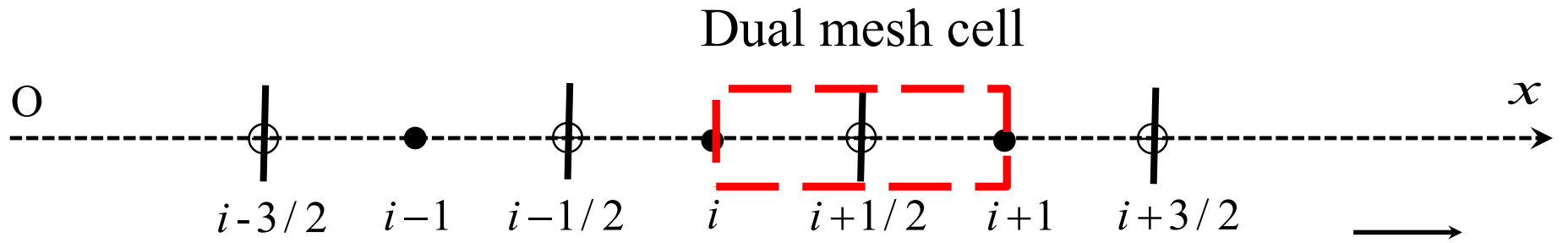
$$(\rho u)_i^{n+1} = (\rho u)_i^n - \frac{\Delta t}{\Delta x} \left[(\rho u)_i^{n+1} A_i - B_i + (p)_{i+1/2}^{n+1} - (p)_{i-1/2}^{n+1} \right]$$

or equivalently:

$$B_i = (\rho u)_i^{n+1} A_i + (p)_{i+1/2}^{n+1} - (p)_{i-1/2}^{n+1} + \frac{\Delta x}{\Delta t} \left[(\rho u)_i^{n+1} - (\rho u)_i^n \right] \text{ or}$$

$$B_i = B_{i+1} + (p)_{i+1/2}^{n+1} - (p)_{i-1/2}^{n+1} + \frac{\Delta x}{\Delta t} \left[(\rho u)_i^{n+1} - (\rho u)_i^n \right]$$

Momentum interpolation method: dual mesh equation



$$B_{i+1/2} \xrightarrow{\quad} \underset{\oplus}{\boxed{V_{i+1/2}}} \xrightarrow{\quad} B_{i+3/2} = A_{i+1/2} \times (\rho u)_{i+1/2}$$

The same type of discretized momentum equation is postulated on the dual mesh, namely:

$$B_{i+1/2} = (\rho u)_{i+1/2}^{n+1} A_{i+1/2} + (p)_{i+1}^{n+1} - (p)_i^{n+1} + \frac{\Delta x}{\Delta t} \left[(\rho u)_{i+1/2}^{n+1} - (\rho u)_{i+1/2}^n \right]$$

Momentum interpolation method: relating primal and dual cells quantities

Where $A_{i+1/2}$ and $B_{i+1/2}$ are for instance supposed to be such that
(Rhee and Chow, 1993, other alternatives possible):

$$A_{i+1/2} = 2 \frac{A_i A_{i+1}}{A_i + A_{i+1}}$$

$$\frac{B_{i+1/2}}{A_{i+1/2}} = \frac{1}{2} \left(\frac{B_i}{A_i} + \frac{B_{i+1}}{A_{i+1}} \right) \text{ which leads to:}$$

$$\begin{aligned} (\rho u)_{i+1/2}^{n+1} &= \frac{1}{2} \left[\frac{(\rho u)_{i-1}^{n+1} u_{i-1/2}^n}{u_{i+1/2}^n} + \frac{(\rho u)_i^{n+1} u_{i+1/2}^n}{u_{i+3/2}^n} \right] - \frac{1}{A_{i+1/2}} \left[(p)_{i+1}^{n+1} - (p)_i^{n+1} \right] \\ &\quad - \frac{1}{A_{i+1/2}} \frac{\Delta t}{\Delta x} \left[(\rho u)_{i+1/2}^{n+1} - (\rho u)_{i+1/2}^n \right] \end{aligned}$$

Momentum interpolation method: the final expression of the primal cell face velocity

$$(u)_{i+1/2}^{n+1} = (\rho u)_{i+1/2}^{n+1} / \rho_{i+1/2}^{n+1} \text{ where } \rho_{i+1/2}^{n+1} = \frac{1}{2} [\rho_i^{n+1} + \rho_{i+1}^{n+1}]$$

and the ρ_i^{n+1} are calculated through the continuity equation discretized as the momentum on the primal mesh.

We are done with the interface velocity on the primal mesh but not with the pressure interface !

The MIAU flux scheme *(Momentum Interpolation with Advection Upwind Splitting)*

It is our latest proposal of a momentum interpolation specifically adapted to a pressure-based predictor-corrector approach for compressible flows with up to second-order accuracy.

The MIAU flux scheme (*Momentum Interpolation with Advection Upwind Splitting*)

1. The face velocity (continued) $v_{i+1/2}^* = \frac{(\varrho v)_{i+1/2}^{**}}{\varrho_{i+1/2}^k}$,

(The kth iteration of the predictor-corrector step is designated by superscript k)

$$B_{i+1/2}^k = A_{i+1/2}^k (\varrho v)_{i+1/2}^{**} + p_{i+1}^k - p_i^k + \frac{\Delta x}{\Delta t} [(\varrho v)_{i+1/2}^{**} - (\varrho v)_{i+1/2}^n]$$

with

$$A_{i+1/2}^k = \frac{1}{2} (A_i^k + A_{i+1}^k), \quad B_{i+1/2}^k = \frac{1}{2} (B_i^k + B_{i+1}^k).$$

$$A_i^k = v_{i+1/2}^{\text{AUSM}^+},$$

$$B_i^k = \left\{ (\varrho v)_{i-1}^k + \frac{1}{2} \psi_{i-1} [(\varrho v)^k] \right\} v_{i-1/2}^{\text{AUSM}^+} - \frac{1}{2} \psi_i [(\varrho v)^k] v_{i+1/2}^{\text{AUSM}^+}$$

The MIAU flux scheme (continued)

(Momentum Interpolation with Advection Upwind Splitting)

1. The face velocity (end)

AUSM+ scheme (Liou, 1996)

$$v_{i+1/2}^{\text{AUSM}^+} = c_{i+1/2} M_{i+1/2}, \quad c_{i+1/2} = \min\{\tilde{c}_L, \tilde{c}_R\},$$

$$\tilde{c}_L = (c_L^*)^2 / \max\{c_L^*, |v_L|\}, \quad \tilde{c}_R = (c_R^*)^2 / \max\{c_R^*, |v_R|\}, \quad (c_{L,R}^*)^2 = \frac{2(\gamma - 1)}{\gamma + 1} H_{L,R},$$

$$M_{i+1/2} = f_M^+(M_L) + f_M^-(M_R),$$

$$\text{with } f_M^\pm(m) = \begin{cases} \frac{1}{2}(m \pm |m|) & , |m| \geq 1, \\ \pm \frac{1}{4}(m \pm 1)^2 \pm \frac{1}{8}(m^2 - 1)^2 & , |m| < 1, \end{cases}$$

$$M_{L,R} = v_{L,R}/c_{i+1/2},$$

The MIAU flux scheme *(Momentum Interpolation with Advection Upwind Splitting)*

2. The face pressure

$$p_{i+1/2} = \frac{1}{2}(p_L + p_R) + \frac{1}{2}f_p \varrho_{i+1/2} c_{i+1/2} (v_L - v_R).$$

This is a characteristic-like expression with a scaling function f_p (Kitamura and Shima, 2011) for ensuring a correct behavior at low Mach.

$$f_p = 2 \widehat{M}_{i+1/2} - \widehat{M}_{i+1/2}^2, \quad \widehat{M}_{i+1/2} = \min \left\{ 1, \sqrt{\frac{v_L^2 + v_R^2}{2c_{i+1/2}^2}} \right\}.$$

The predictor step

- $p_i^* = p_i^k$

- ϱ_i^* from

$$\begin{aligned} \frac{1}{\Delta t}(\varrho_i^* - \varrho_i^n) + \frac{1}{\Delta x} & \left[\varrho_i^* + \frac{1}{2}\psi_i(\varrho^k) \right] v_{i+1/2}^* \\ & - \frac{1}{\Delta x} \left[\varrho_{i-1}^* + \frac{1}{2}\psi_{i-1}(\varrho^k) \right] v_{i-1/2}^* = 0 \end{aligned}$$

- $(\varrho v)_i^*$ from

$$\begin{aligned} \frac{1}{\Delta t} & [(\varrho v)_i^* - (\varrho v)_i^n] + \frac{1}{\Delta x} \left\{ (\varrho v)_i^* + \frac{1}{2}\psi_i[(\varrho v)^k] \right\} v_{i+1/2}^* \\ & - \frac{1}{\Delta x} \left\{ (\varrho v)_{i-1}^* + \frac{1}{2}\psi_{i-1}[(\varrho v)^k] \right\} v_{i-1/2}^* + \frac{1}{\Delta x} (p_{i+1/2}^k - p_{i-1/2}^k) = 0 \end{aligned}$$

- $(\varrho E)_i^* = \frac{p_i^k}{\gamma - 1} + \frac{1}{2} \frac{[(\varrho v)_i^*]^2}{\varrho_i^*} , \quad (\varrho H)_i^* = (\varrho E)_i^* + p_i^k , \quad h_i^* = \frac{\gamma}{\gamma - 1} \frac{p_i^k}{\varrho_i^*}$

The correction step

- $\varrho^{k+1} = \varrho^*$.
- $p' = p^{k+1} - p^k$ from

$$C_{i-1}p'_{i-1} + C_i p'_i + C_{i+1} p'_{i+1} = -\Sigma_i,$$

where, with the notation $\tau = \Delta t / \Delta x$,

$$C_{i-1} = -\tau \frac{\gamma}{\gamma - 1} v_{i-1/2}^* - \tau \alpha_{i-1/2}^k h_{i-1}^*,$$

$$C_i = \frac{1}{\gamma - 1} + \tau \frac{\gamma}{\gamma - 1} v_{i+1/2}^* + \tau \left(\alpha_{i+1/2}^k h_i^* + \alpha_{i-1/2}^k h_{i-1}^* \right),$$

$$C_{i+1} = -\tau \alpha_{i+1/2}^k h_i^*,$$

$$\begin{aligned} \Sigma_i &= [(\varrho E)_i^* - (\varrho E)_i^n] + \tau \left\{ \frac{1}{2} \frac{[(\varrho v)_i^*]^2}{\varrho_i^*} + \frac{1}{2} \psi_i \left(\frac{1}{2} \frac{[(\varrho v)^k]^2}{\varrho^k} \right) \right\} v_{i+1/2}^* \\ &\quad - \tau \left\{ \frac{1}{2} \frac{[(\varrho v)_{i-1}^*]^2}{\varrho_{i-1}^*} + \frac{1}{2} \psi_{i-1} \left(\frac{1}{2} \frac{[(\varrho v)^k]^2}{\varrho^k} \right) \right\} v_{i-1/2}^* \\ &\quad + \tau \left\{ (\varrho h)_i^* + \frac{1}{2} \psi_i [(\varrho h)^k] \right\} v_{i+1/2}^* - \tau \left\{ (\varrho h)_{i-1}^* + \frac{1}{2} \psi_{i-1} [(\varrho h)^k] \right\} v_{i-1/2}^*. \end{aligned}$$

Updates

$$\varrho_i^{k+1} = \varrho_i^*,$$

$$p_i^{k+1} = p_i^k + p'_i,$$

$$(\varrho v)_i^{k+1} = (\varrho v)_i^* + (\varrho v)'_i = (\varrho v)_i^* - \alpha_i^k (p'_{i+1/2} - p'_{i-1/2}),$$

$$(\varrho E)_i^{k+1} = (\varrho E)_i^* + \frac{1}{\gamma - 1} p'_i$$

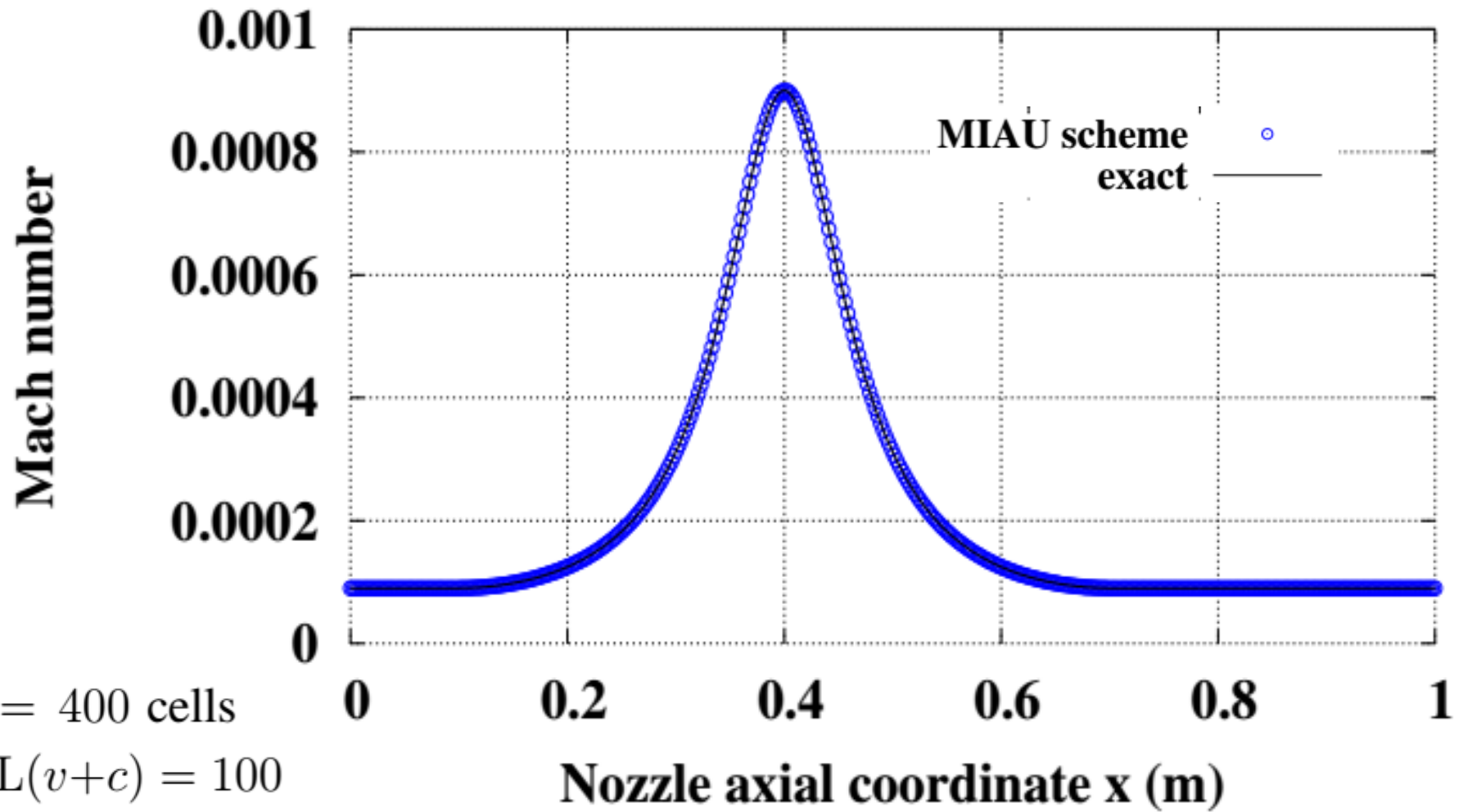
with

$$p'_{i+1/2} = \frac{1}{2}(p'_i + p'_{i+1}) \quad \text{and} \quad \alpha_i^k = \frac{1}{\frac{\Delta x}{\Delta t} + A_i^k}.$$

A few k-iterations are sufficient to converge the loop.

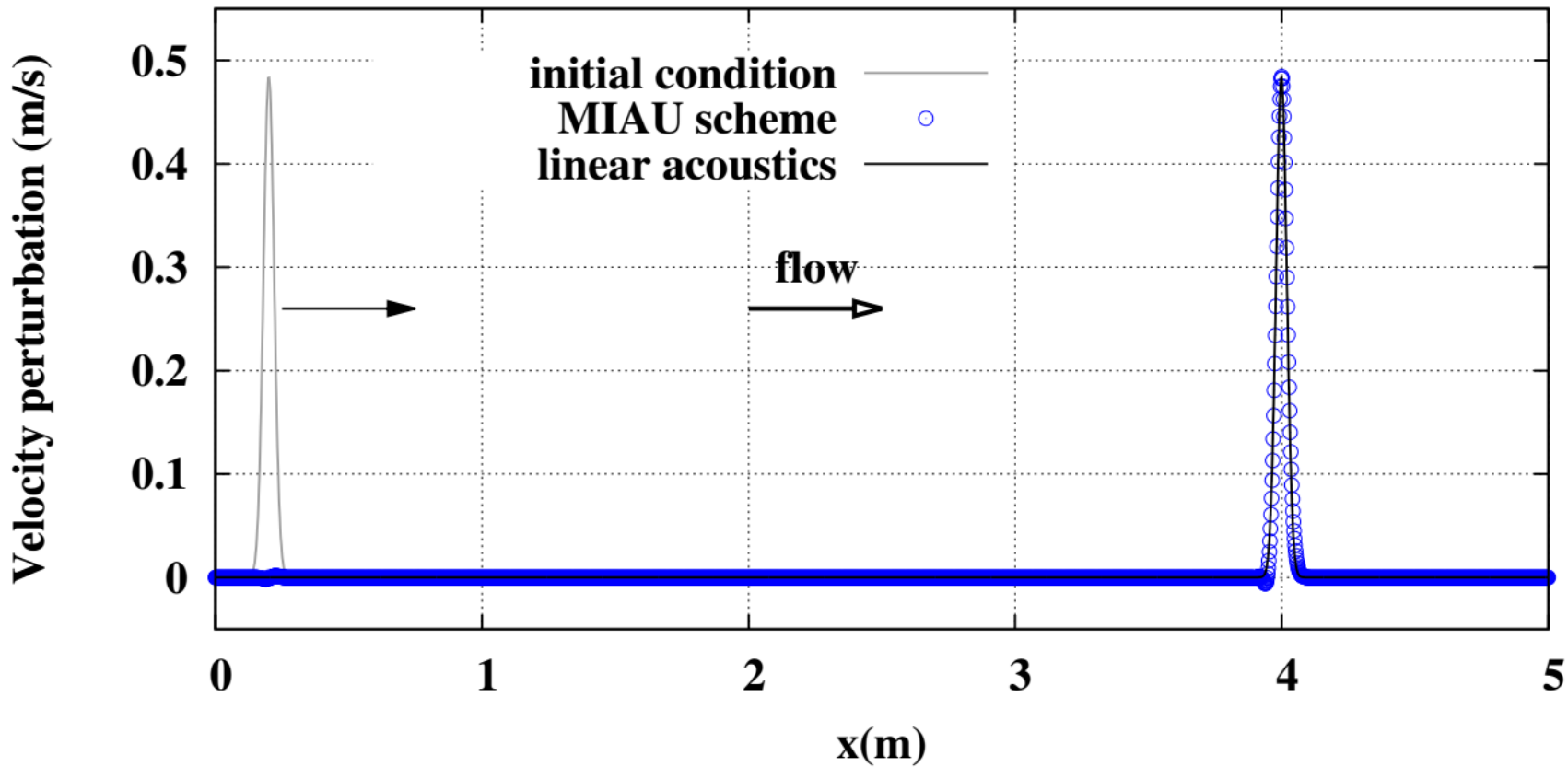
A few results (From Moguen et al., 2018)

Low Mach flow configuration: nozzle flow



Low Mach flow configuration: acoustic pulse (1D)

$$\text{CFL}(v_0 + c_0) = 0.5 \quad 2 \text{ 500 cells} \quad (\delta p)^0 = 200 \exp\left[\frac{(x - 0.2)^2}{2\sigma^2}\right] \text{ (Pa)}, \quad \sigma = 2 \times 10^{-2} \text{ m},$$

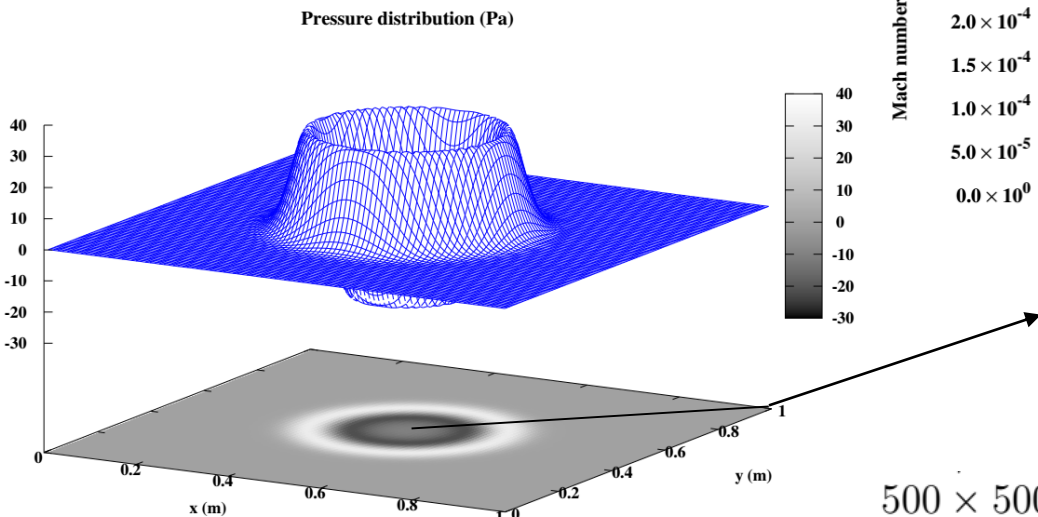


$$\begin{aligned} \varrho^0 &= \varrho_0 + (\delta\varrho)^0, & v^0 &= v_0 + (\delta v)^0, & p^0 &= p_0 + (\delta p)^0, & v_0 &= 3.0886 \times 10^{-2} \text{ m/s} \\ (\delta\varrho)^0 &= (\delta p)^0/c_0^2, & (\delta v)^0 &= (\delta p)^0/(\varrho_0 c_0), & \text{with } c_0 &= \sqrt{\gamma p_0/\varrho_0}. & p_0 &= 101300 \text{ Pa} \\ & & & & & \varrho_0 &= 1.2046 \text{ kg/m}^3 \end{aligned}$$

Low Mach flow configuration: acoustic pulse (2D)

$t_f = 0.5 \text{ ms.}$

$p - p_{\text{out}}$ (Pa)

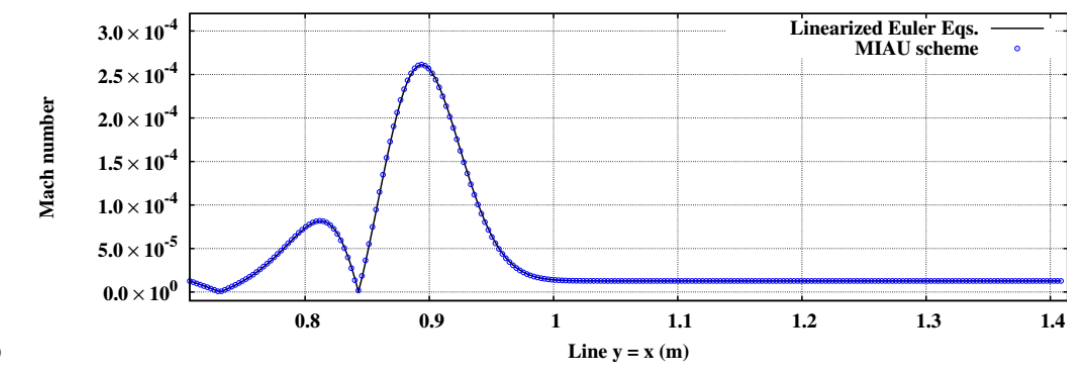
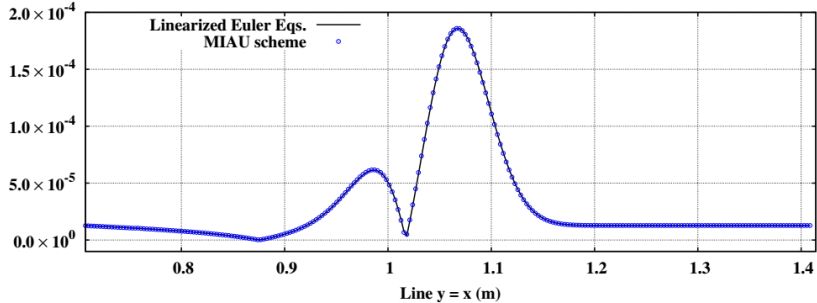


500×500 cells

$$\varrho_0 = 1.2046 \text{ kg/m}^3, u_0 = v_0 = 3.0886 \times 10^{-3} \text{ m/s}, p_0 = 101300 \text{ Pa},$$

$t_f = 1 \text{ ms.}$

Mach number



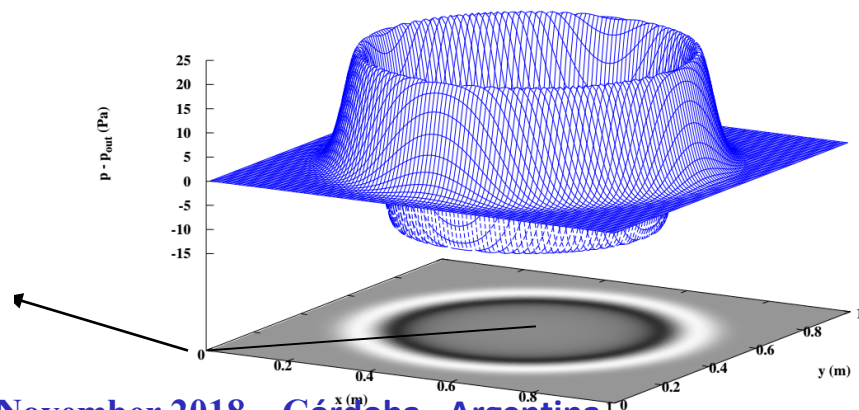
$$(\delta p)^0 = A \exp \left\{ -\alpha [(x')^2 + (y')^2] \right\} (\text{Pa}),$$

with $A = 200$, $\alpha = 1/(0.05)^2$, $x' = x - 0.5$, $y' = y - 0.5$,

$$(\delta \varrho)^0 = (\delta p)^0 / c_0^2 \text{ and } c_0 = \sqrt{\gamma p_0 / \varrho_0}.$$

$$\text{CFL}(v_0 + c_0) = 5$$

Pressure distribution (Pa)

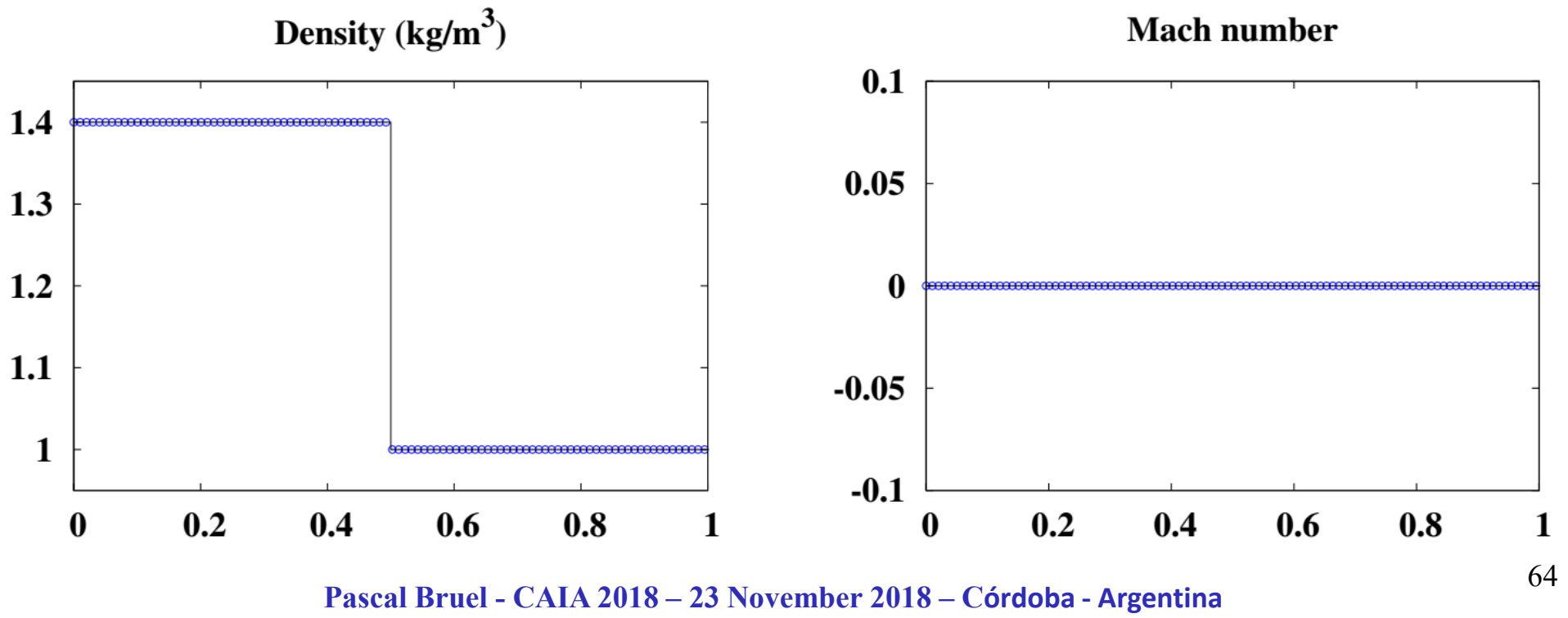


63

Low Mach flow configuration: stationary contact discontinuity

ϱ_L (kg/m ³)	v_L (m/s)	p_L (Pa)	ϱ_R (kg/m ³)	v_R (m/s)	p_R (Pa)	t_f (s)
1.4	0	1	1.0	0	1	100

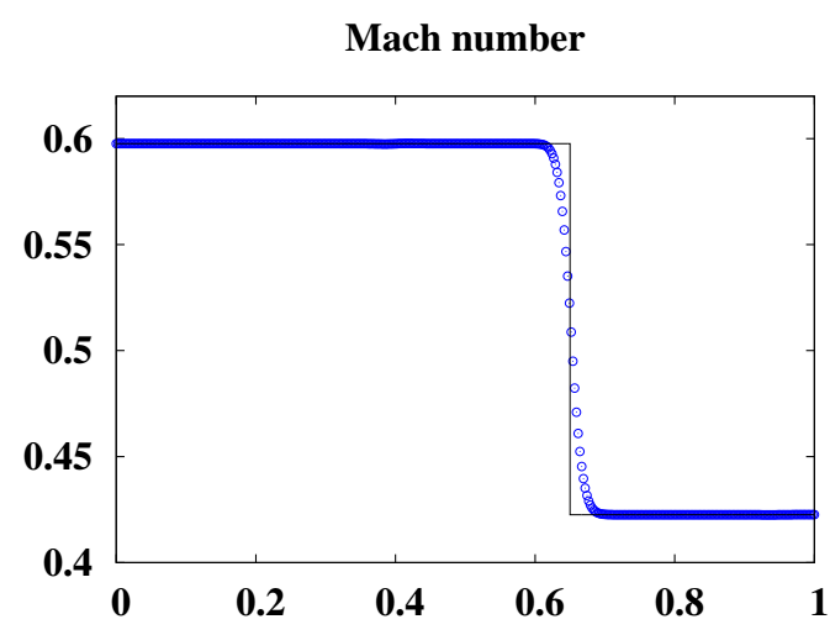
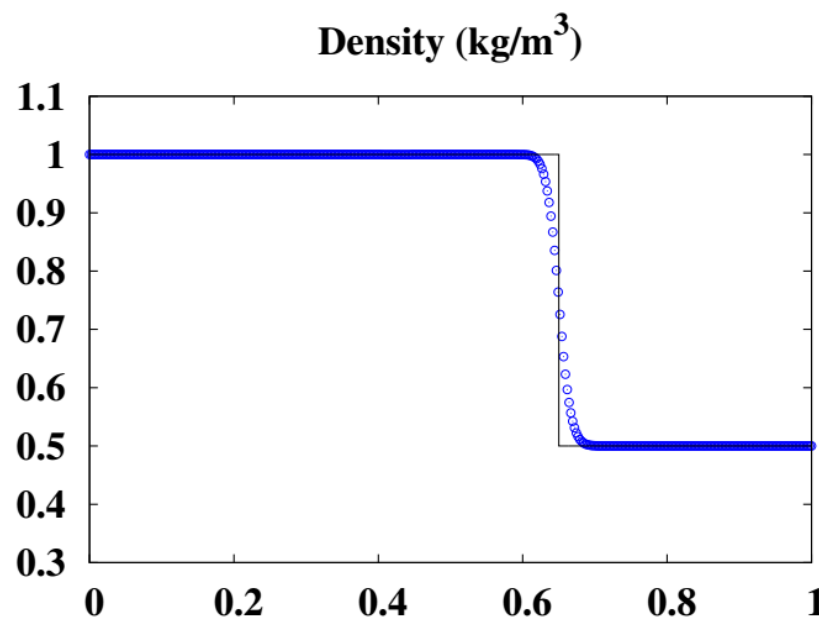
$N = 200$ cells and $CFL(c_L) = 0.5$



Low Mach flow configuration: moving discontinuity

ϱ_L (kg/m ³)	v_L (m/s)	p_L (Pa)	ϱ_R (kg/m ³)	v_R (m/s)	p_R (Pa)	t_f (s)
1	0.5	0.5	0.5	0.5	0.5	0.3

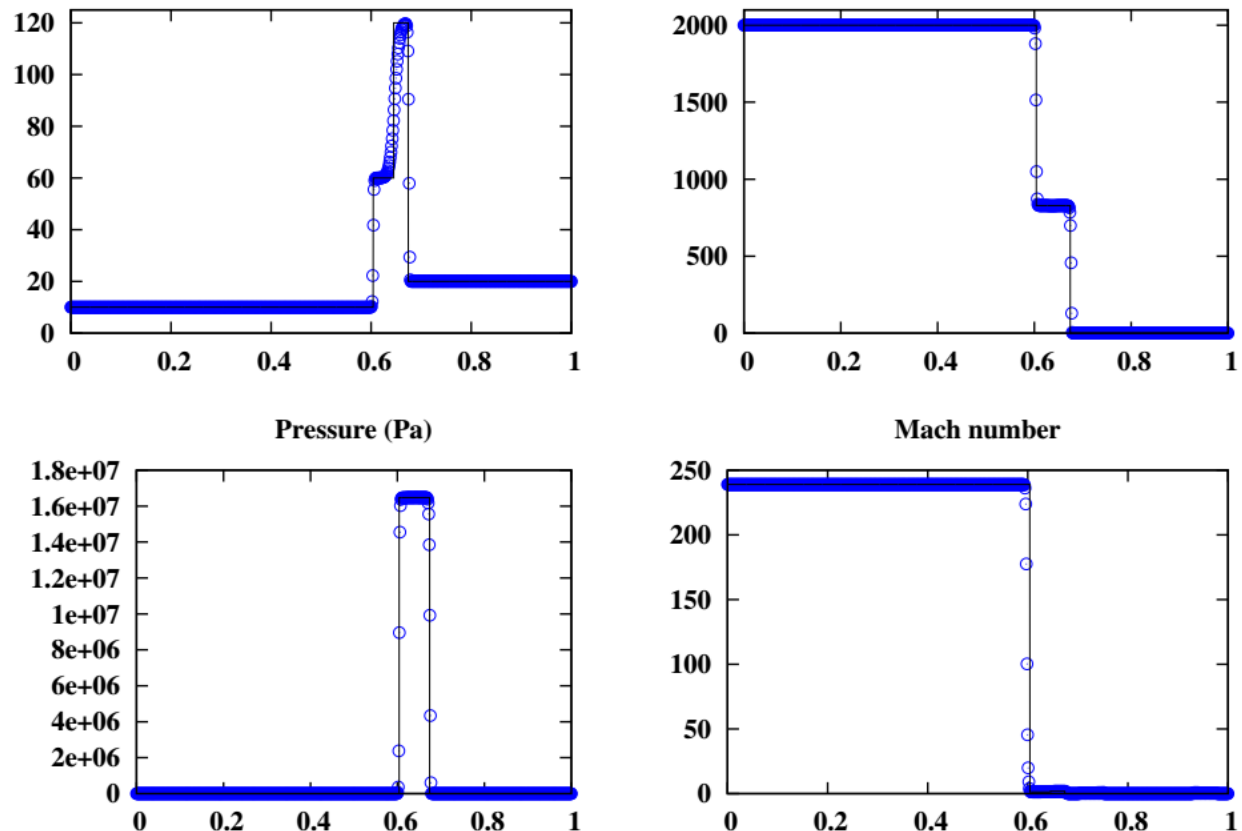
$N = 400$ cells, CFL = 0.4



High Mach flow configurations also : very high Mach shock tube

ϱ_L (kg/m ³)	v_L (m/s)	p_L (Pa)	ϱ_R (kg/m ³)	v_R (m/s)	p_R (Pa)	t_f (s)
10	2 000	500	20	0	500	1.75×10^{-4}

$N = 800$ cells and $\text{CFL}(v_L) = 0.5$.



Conclusion

- A parameter free pressure-based method has been presented
- It has been developed for a colocated finite volume approach.
- The maximum order of accuracy is two.
- It proved to be versatile: low to high Mach flows, smooth or not.

Some interesting references

H. Guillard and B. Nkonga (2017) “*On the behaviour of upwind schemes in the low Mach number limit: a review*”. Handbook of Numerical Analysis, **18**:203-231.

S. Klainerman and A. Majda (1981) “*Singular limits of quasilinear hyperbolic systems with large parameters and the incompressible limit of compressible fluids*”. Communications on Pure and Applied Mathematics, **34**(4):481-524.

R. Klein (1995) “*Semi-implicit extension of a Godunov-type scheme based on low Mach number asymptotics I: one-dimensional flow*”. Journal of Computational Physics, **121**:213-237.

B. Müller (1999) “*Low-Mach number asymptotics of the Navier-Stokes equations and numerical implications*”. In 30th Computational Fluid Dynamics Lecture Series, von Karman Institute for Fluid Dynamics, 8-12 March.

C.-N Xiao, F. Denner and B.G.M. van Wachem (2017) “*Fully-coupled pressure-based finite-volume framework for the simulation of fluid flows at all speeds in complex geometries*”. Journal of Computational Physics, **346**:91-130.

Gracias por su atención